Exploring Exogenous Matrix Metalloproteinases for Regulating Tendon Formation in Tissue Engineered Collagen Scaffolds

A Thesis
Presented in Partial Fulfillment of the Requirements for the
Degree of Master of Science
with a
Major in Biological Engineering
in the
College of Graduate Studies
University of Idaho
by

Mareyna M. Karlin

Major Professor: Nathan Schiele, Ph.D.
Committee Members: Matthew Bernards, Ph.D.; Bryn Martin, Ph.D.
Department Administrator: Ching-An Peng, Ph.D.

May 2020

Authorization to Submit Thesis

This thesis of Mareyna M. Karlin, submitted for the degree of Master of Science with a Major in Biological Engineering and titled “Exploring Exogenous Matrix Metalloproteinases for Regulating Tendon Formation in Tissue Engineered Collagen Scaffolds,” has been reviewed in final form. Permission, as indicated by the signatures and dates below, is now granted to submit final copies to the College of Graduate Studies for approval.

Major Professor: _____ Date: _____
Nathan Schiele, Ph.D.

Committee Members: _____ Date: _____
Matthew Bernards, Ph.D.

_____ Date: _____
Bryn Martin, Ph.D.

Department
Administrator: _____ Date: _____
Ching-An Peng, Ph.D.

Abstract

Tendon is one of the most commonly injured musculoskeletal tissues. Developing methods for regenerating tendon tissue will be crucial for the future treatment of tendon injuries. Tissue engineering strategies have explored combining cells, scaffolds, and signals for guiding tissue formation. Potential signals include biochemical and mechanical factors, but there is a need to identify appropriate combination of signals that regulate tendon formation. Recently, the enzymes that degrade matrix proteins, matrix metalloproteinases (MMPs), have been found in developing tendons. However, their use in engineered tendon formation has been limited. Therefore, our overall objective was to explore the combination of exogenous MMPs and mechanical strain to understand their roles in regulating engineered tendon tissue formation *in vitro*. In the following chapters we examine how mesenchymal stem cells (MSCs) and collagen type I scaffolds were impacted by MMPs and mechanical stimulus. We tested our central hypothesis that the alignment of the collagen fibers in the scaffolds would be improved with the combination of MMPs and tensile strain. In Chapter 2, treatments with exogenous pro-form MMP-1, 2, 8, and 13 were used to determine impacts on collagen scaffolds and MSCs. In Chapter 3, collagen scaffolds and tenogenically induced MSCs were treated with exogenous active MMP-1, 2, 8, and 13. In Chapter 4, exogenous active MMP-1, 2, 8, and 13 treatments in combination with a tensile strain were explored. The results of these studies showed that MMPs do not negatively impact MSC growth and viability. Furthermore, exogenous MMP treatments alone did not show any significant trends in collagen alignment, but the addition of a tensile strain in combination with active MMPs indicated that some localized collagen alignment occurred. This work provides important preliminary data for future tissue engineering studies and suggests that MMPs, mechanical loading, and their combinations may have promise for improving engineered tendon formation.

Acknowledgements

A special thanks to Nate Schiele for the advisement and countless learning opportunities. Thanks to Sophia Theodossiou for her time spent in the lab helping with experiments, and Nicholas Pancheri and Annie Carper for their hours spent on the confocal microscope. Thank you to William Miller for writing a program to complete the image post processing and offering programming advice and assistance. Thank you to Jeff Preston for statistics help. We also would like to acknowledge funding for this work from the NIH/NIBIB (R03EB024134).

Dedication

I would like to dedicate this to the family and friends who lovingly and patiently supported me through the entirety of my academic career. I would also like to dedicate this to Susie Johnson and Kaitlyn Preston, who were always bright spots in my day, making life feel a little less overwhelming when things felt too hard.

Table of Contents

List of Tables

List of Figures

Chapter 1: Tendon Tissue Engineering Introduction and Background

Musculoskeletal injuries are the second largest contributors to disability (1). As many as 20-33% of people worldwide struggle with a musculoskeletal injury (1). Tendons are an important component of the musculoskeletal system (2). They transmit forces from muscular contractions between the muscle and bone (2, 3) which allows for movement and range of motion that are necessary for normal function. Tendons are composed of tendon cells within an extracellular matrix (ECM) (2). The ECM is composed mainly of collagen, elastin, proteoglycans, and water. The collagen is highly organized and is the main structural component of tendons. It is arranged into fibrils, fibers, and fascicles, as shown in Figure 1.1 (1). This structure is important for the mechanical properties of tendons (2, 4, 7). These collagen fibrils are aligned along the tendon long axis, giving tendons mechanical properties that allow movement (2, 7). The water and proteoglycans may help the collagen fibers slide past one another.

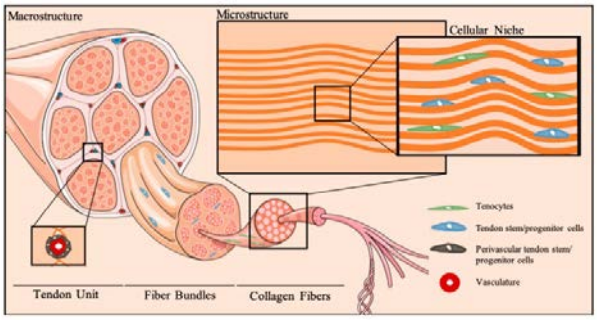

Figure 1.1: Tendon structure and composition (1)

Tendon injuries are very common, contributing to the annual 15 million musculoskeletal injuries in the United States (5). While these injuries are common in athletes, they are also increasingly common in the general population. Injured tendons do not heal or regenerate well (3). One common form of tendon injury is tendinopathy. Tendinopathy is painful and can cause collagen disorganization, overexpressed fibrillar collagen, and changed fibroblast morphology (8). This leads to changes in normal structure and mechanical function. An important component of tendon composition is collagen type I that is organized in an aligned pattern. After injury, this collagen becomes disorganized. This disorganization causes changes to the mechanical properties that tendons need to be functional tissue. As a result, range of motion becomes limited and the injured individual can experience significant pain, discomfort, and a decreased quality of life. Since tendons have poor regenerative capabilities, surgical intervention is often used (9). The goal is to alleviate pain by attempting to restore the tendon back to normal tissue (9). Surgical intervention is the most common tendon repair method and involves suturing the two ends of the torn tendon back together. Since tendon is a fibrous tissue composed primarily of organized collagen type I (10, 43), this is not a sufficient repair and suturing is even more difficult if scar tissue and disorganized collagen are present.

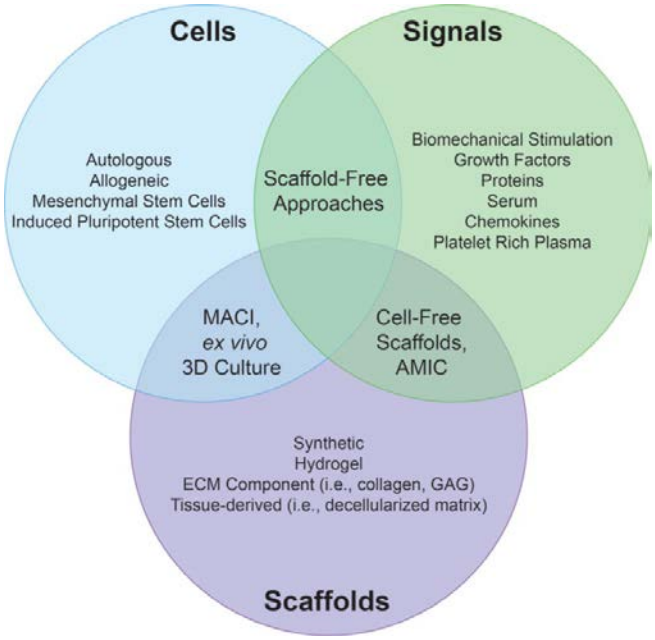

Figure 1.2: Tissue Engineering Paradigm (12)

Many repaired tendons are incapable of returning to their pre-injury state (1). As a result, a functional tendon replacement is needed. Promising fields of research to find a suitable tendon replacement are regenerative medicine and tissue engineering. Regenerative medicine includes tissue engineering and incorporates the idea of self-healing using what is already there. Tissue engineering is then the development of biological substitutes used to restore, maintain, and improve tissue function (11). The consideration is then what components can be used to make tissue. One way of thinking about this is through the Tissue Engineering Paradigm in Figure 1.2 (12), which considers many combinations of cells, scaffolds, and signals to try and mimic the tissue's natural environment. The use of these methods will be imperative for developing a functional tissue repair method or replacement.

There are many cell considerations for tendon tissue engineering, and cells have shown to be very important in methods of tissue regeneration (1). Each cell type has its own advantages and disadvantages. Mesenchymal Stem Cells (MSCs) are commonly used for tendon tissue engineering (1) and are important to normal tissue growth and maintenance (1,13). Though there is no standardized protocol for tenogenically differentiating MSCs, they are still commonly used in tissue engineering, as they are readily available, multipotent, and available for musculoskeletal differentiation (5). These cells have been shown to differentiate into cartilage, bone, fat, muscle, tendon, and skin (13). Some of the MSC differentiation capabilities are shown in Figure 1.3. They have demonstrated the ability to accelerate and improve tendon healing through assisting the biological response to injury (1, 13). Using these cells for tendon research and treatments is promising as they can provide an alternative to using tendon cells which are in short supply and would result in further tendon injury (e.g., donor site morbidity) (1). However, being able to control the differentiation of MSCs into functional tendon cells is challenging and will be necessary (42, 46). Several groups have explored the combination of MSCs and biomaterial scaffolds to address this issue, but there is still research to be done (1).

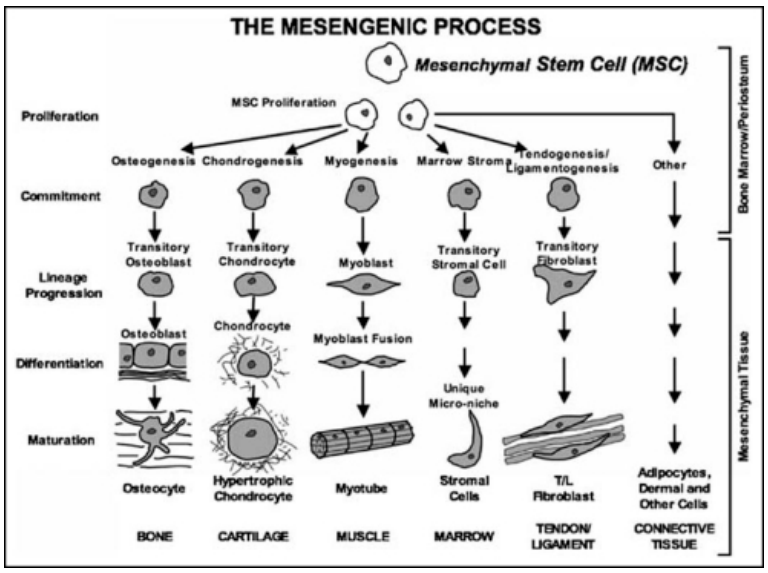

Figure 1.3: The many differentiation capabilities of MSCs (13).

Scaffolds are the next component of the tissue engineering paradigm. There are many types of scaffolds varying from natural to synthetic and they can be made of one or multiple types of materials, with some examples being alginate hydrogels and collagen scaffolds (54, 55). Collagen scaffolds are commonly used because of their porous structure, permeability, and biodegradability. These properties help regulate cell morphology, adhesion, migration, and differentiation (9). Collagen is one of the most abundant proteins in the extracellular matrix and is one of the main structural proteins in humans (9). Scaffolds composed of collagen type I, the main protein component in tendon, have been explored for tendon tissue engineering because of these reasons (8, 33, 4).

The final area of the tissue engineering paradigm is signaling. Signals are an important aspect of tissue development and function and can help further mimic a tissue's natural environment. Some important signals for tendon development and repair are biochemical signals and mechanical signals. Biochemical signals include various enzymes and growth factors, while mechanical signals include different types of mechanical loading. All these signals are used to regulate tenogenesis, and tendon healing (1). Some of these signals include cytokines, growth factors, and bone morphogenic proteins (1). One of the main growth factors involved in tenogenesis is transforming growth factor beta 2 (TGFβ2) (3, 35, 36). Enzymes may also be essential signals in tendon formation. Matrix metalloproteinases (MMP) are enzymes that can degrade collagen, ECM, and non-matrix proteins (16). MMPs are likely to play a role in tendon formation, healing, and regeneration (18, 19, 23). Mechanical stimulus is also an important consideration, as mechanical

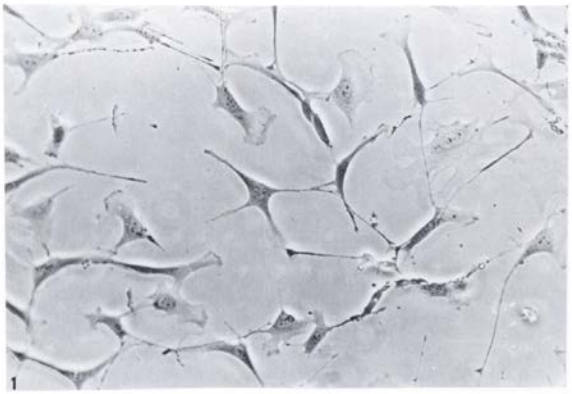

Figure 1.4: C3H10T1/2 Mesenchymal Stem Cells (14).

loading is necessary for tendon formation (5). Each of these potential signals will be discussed in more detail below.

One family of growth factors, TGFβs, are important cellular regulatory factors (14). The TGFβ family regulates several processes such as apoptosis, fibrosis, differentiation, and inflammation (14). TGFβ2 is a promising biochemical tenogenic regulatory factor, as it is present in developing tendons (3, 10). TGFβ2 induces MSCs to become more fibroblastic, a similar cell morphology to tendon cells found in healthy tendons (3, 5, 44). The addition of TGFβ2 to MSCs promotes differentiation and commitment to the tendon cell lineage (tenogenesis), demonstrated by an increase in tendon markers, such as scleraxis and tenomodulin (3, 10). In developing embryonic chickens, TGFβ2 treatment in the limb induced the expression of the tendon marker scleraxis (16). The TGFβ2 pathway also seems to play an important role in collagen type I and III regulation and expression (8). The combination of TGFβ2 and other factors may further promote tenogenesis *in vitro*. TGFβ2 is also believed to play a role in tendon healing (1).

An underexplored regulator of tendon tissue formation and tenogenesis is MMPs. MMPs are zinc and calcium dependent enzymes that degrade collagen, ECM, and non-matrix proteins (16). These degradative properties are involved in tissue development, repair, and remodeling (18, 19). In damaged and developing tissue, inflammatory factors and resident tendon cells produce MMPs for tissue breakdown and remodeling (8, 18). MMPs have been shown to be important in the bone remodeling process (19) and could also be important in tendon healing and development.

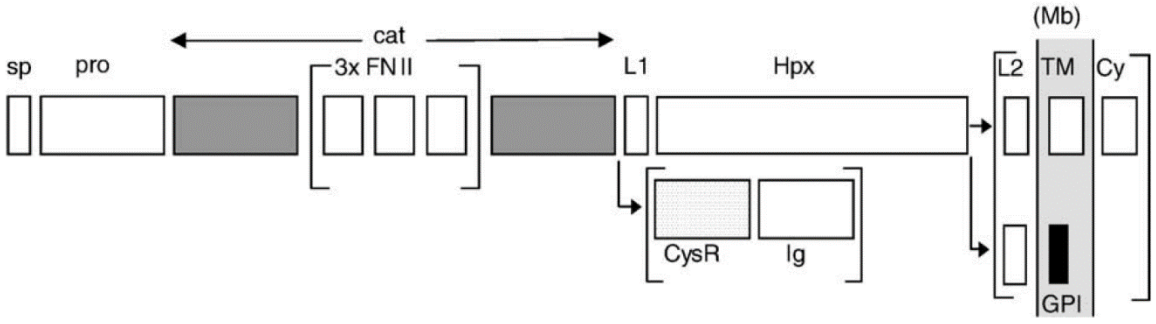

Figure 1.5: MMP Structure shown through the multiple domains (18).

In addition, MMPs have a zinc-based structure and are composed of multiple domains: a pro-domain, a catalytic domain, and a hemopexin domain, seen in Figure 1.5 (16, 18). MMPs are either in pro-form or active form, and MMP activation depends on the specific structure. Activation from the pro-form is a highly regulated, stepwise process (16, 18). For activation to occur, the pro domain must either be cleaved or displaced from the catalytic domain (16, 18). This activation can occur through proteolytic cleavage where the pro domain is removed, or allosteric activation where the pro domain is displaced (16). *In vivo*, activation may take place under a number of conditions including inflammation, and MMP activity is controlled by factors such as membrane tethered MMPs (MT-MMPs) and trypsin (8, 18). MMP activity is regulated at multiple levels through activation, inhibition, complex formation, and compartmentalization (16). Whichever mechanism activation occurs through, the pro domain needs to be physically delocalized from the catalytic site (16). *Ex vivo*, compounds like 4 Aminophenylmercuric acetate (APMA) and serine proteinases can be added to activate MMPs (20). Once the pro domain is cleaved, the MMP structure has an open binding site where the pro-domain used to be (18). This open binding site allows binding to molecules for degradation. For some MMPs, activation is necessary for the binding of collagen type I.

There are multiple types of MMPs including collagenases, gelatinases, stromelysins, matrilysins, and MT-MMPs (18). MMPs are actively involved in the healing process as they degrade and remodel ECM (7). Since tendons are made of collagen, it is likely that MMPs remodel tendons as well. MMP-1, 2, 8, and 13 are often found in injured tendon (24). These MMPs likely play a large role in the healing and remodeling of the tendon tissue. MMP-1, MMP-8, and MMP-13 are collagenases and cleave interstitial collagens I, II, & III into fragments and cleave ECM molecules and soluble proteins. MMP-2 is a gelatinase and digests gelatin and ECM molecules (18). It has been shown to be at high levels during embryonic tendon development (23, 37, 38). Collagenases typically degrade whole collagen molecules while gelatinases degrade smaller networks of collagen (8). Collagenases degrade collagen through binding to the collagen's triple helices at the surface and digesting the collagen fibrils from the inside out (9).

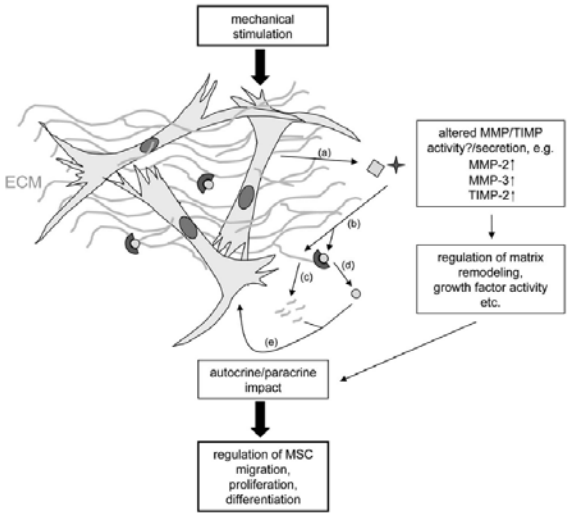

Figure 1.6: Effects of mechanical stimulation on MSCs (19)

Mechanical loading is another important signal for tendon formation. Physical forces from contracting muscles are necessary for normal tendon development and maintenance (39, 40, 41). Since tendons act as force transmitters, they are sensitive to loading (16). Loading is therefore important for developing and maintaining a healthy musculoskeletal system and promoting tenogenesis (20). It has been shown in developing chicks that mechanical forces are required for formation of the skeletal system (16). Proliferation and differentiation of MSCs are also influenced by loading, as well as expression of tenogenic markers (19, 45). MMP production by MSCs may be sensitive to loading, demonstrated in Figure 1.6 (16, 19). MSCs respond to loading through the production of MMPs, ECM proteins (e.g., collagen), and other biochemical factors, and as a result biomechanical properties may be impacted (16, 47, 48, 49). Increases in stiffness, cross sectional area, and tensile strength are found with mechanical stimulation, as well as increased vascularization, seen in Figure 1.7 (20). In *in vivo* studies, tendon that had undergone intense running had a higher expression of tendon related genes (20). In mice that were treated with Botox to unload their tendons, mechanical loading was found to be essential for the maintenance of viscoelastic properties (22). In a different study, unloaded tendons had decreases in tendon markers such as scleraxis (16).

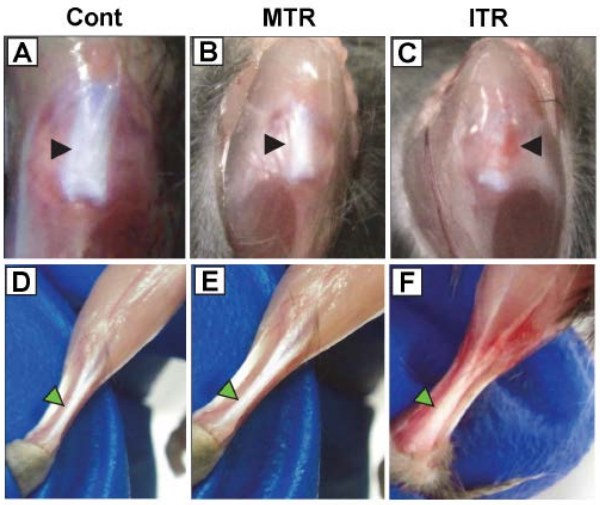

Figure 1.7: Mice tendons after treadmill running (21). The control group is on the left (Cont), The Moderate Treadmill Running (MTR) group is in the middle, and Intensive Treadmill Running (IRT) group is on the right.

Mechanical loading may also play a role in aligning collagen and protecting the collagen from enzymatic degradation by a mechanism known as *Strain Protection* (7, 52, 53). In collagen treated with active MMP-8 and mechanically stretched, the collagen was more preserved by enzymatic degradation, suggesting the importance of combining MMPs with applied strain (7, 52). The degradation rate by MMP-8 was reduced with mechanical loading, seen in Figure 1.8 (7). In a different study, decellularized pericardium was mechanically strained and treated with bacterial collagenase (25). The collagen fiber alignment in the collagenase-treated pericardium matched the direction of strain (25). The unaligned collagen fibers (e.g., fibers that were not aligned with the stretch direction) may have been more easily digested because they were not mechanical loaded (e.g.,

not strain protected) (7, 25). However, these strain studies have been conducted without cells needed in typical tissue engineered scaffold, and have used only MMP-8 or bacterial collagenase (7, 25, 52). Strain protection presents a potential mechanism to improve collagen alignment in collagen scaffolds, whereby combining MMPs and mechanical stretching may preserve collagen fibers aligned with the stretch direction while unaligned fibers may be degraded. However, this has not yet been explored for tendon tissue engineering.

A tissue engineered construct not only needs to be developed using appropriate mechanical stimulation, it also needs to be able to withstand similar forces to normal tendon. Mechanical loading alone does not upregulate most tendon markers (5), which helps demonstrate the need for additional biochemical factors (such as TGFβ2 and MMPs). Tissue engineering is a challenging undertaking, as there are many variables and potential interactions between variables. Tendon tissue engineering presents its own challenges, as it is a relatively new and emerging field and there is still much to be discovered. Though a functional tendon replacement may still be far away, following the tissue engineering paradigm provides a way to better understand the environment needed to accomplish this challenge. In the following chapters we examined how MSCs and collagen type I scaffolds were impacted by MMPs and mechanical stimulus. We tested our central hypothesis that the alignment of the collagen fibers in the scaffolds would be improved with the combination of MMPs and tensile strain. In Chapter 2, treatments with exogenous pro-form MMP-1, 2, 8, and 13 were used to determine impacts on collagen scaffolds and MSCs. In Chapter 3, collagen scaffolds and tenogenically induced MSCs were treated with exogenous active MMP-1, 2, 8, and 13. In Chapter 4, exogenous active MMP-1, 2, 8, and 13 treatments in combination with a tensile strain were explored. Results of these studies showed that MMPs do not negatively impact MSC growth and viability. Furthermore, exogenous MMP treatments alone did not show any significant trends in collagen alignment, but the addition of a tensile strain in combination with active MMPs indicated that localized collagen alignment occurred. This work

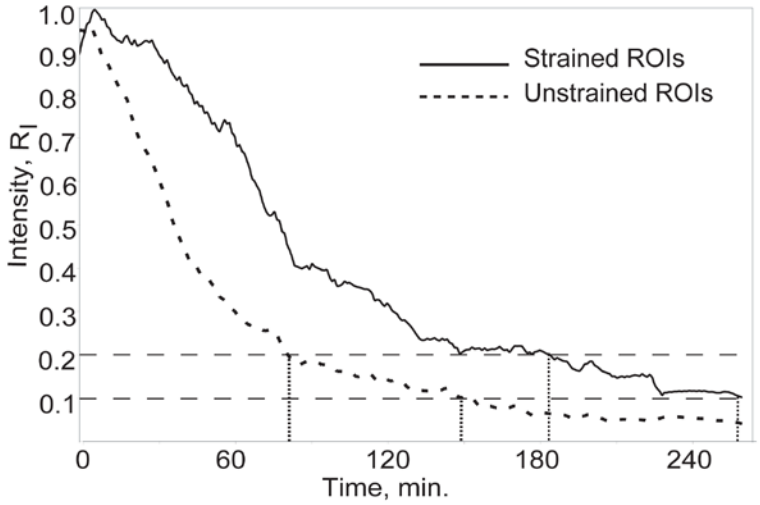

Figure 1.8: Comparison of normalized edge intensity vs time with loaded and unloaded collagen fibrils (7). MMP-8 was added to each set of collagen fibrils prior to straining. Strained collagen fibrils with MMP-8 have a slower degradation rate (7).

provides important preliminary data for future tissue engineering studies and suggests that MMPs, mechanical loading, and their combinations may have promise for improving engineered tendon formation.

Chapter 2: Impact of Pro-form Matrix Metalloproteinases on Mesenchymal Stem Cells and Collagen Type I Scaffolds

Introduction

Tendons are collagenous tissue that connect muscles to bone. Tendon repair and regeneration is needed because tendons have poor healing capability. One typical and promising tendon tissue engineering strategy is the use of mesenchymal stem cells (MSCs) seeded into collagen type I scaffolds (26). However, a major challenge with these collagen scaffolds for tendon replacement is that the collagen network is not aligned or organized, which reduces its mechanical strength and limits the tenogenic cues available to the MSCs. Therefore, we propose exploring treatment with exogenous matrix metalloproteinases (MMP) in combination with MSCs to encourage collagen remodeling and develop more aligned collagen networks within collagen scaffolds. Currently, MMPs have not been widely used in tendon tissue engineering, but could play a pivotal role in tendon tissue formation based on prior studies identifying MMPs in embryonic tendon, and using collagenase to improve collagen alignment in pericardium (23).

MMPs are enzymes that degrade collagen and remodel the extracellular matrix (ECM) (18). There are 24 MMPs found in humans (27). The two major categories of MMPs considered here are collagenases and gelatinases. In the pilot project described in this chapter, we used MMPs 1, 8, and 13 to serve as the collagenases and MMP-2 to serve as the gelatinase. Using collagenases and gelatinases allowed us to see the different effects the two classes of MMPs may have on MSCs in a collagen type I environment.

The objective of this study was to determine how pro-form MMPs impacted MSC growth and the collagen fibers of a tissue engineered tendon scaffold. Here, pro-form MMPs were used to treat MSCs grown in commercially available collagen type I scaffolds. Initially pro-form MMP-1, 2, 8, and 13 were selected to treat MSCs and check for any signs of cytotoxicity. This was done by seeding MSCs into 24 well plates and treating them with varying concentrations of MMP-1, 2, 8, and 13 for 7 days. Pro-form MMPs were then exogenously added to the culture medium of MSCs seeded into collagen scaffolds and cultured for 3 days to observe the changes to the collagen structure. Second harmonic generation (SHG) imaging was used to visualize the collagen network, and images were analyzed to determine collagen network alignment. We predicted that the pro-MMPs in combination with the MSCs would alter the collagen network.

Materials and Methods

Cell Culture

Mouse C3H10T1/2 MSCs were purchased from American Type Culture Collection (ATCC, Manassas VA), expanded using our standard cell culture protocols and growth medium (Dulbecco's Modified Eagle's Medium (DMEM), 10% fetal bovine serum (FBS), and 1% Penicillin/ Streptomycin), and passaged every three to four days. MSCs were seeded at 5,000 cells/cm^2 into 24-well plates and 1,000,000 MSCs per scaffold were seeded into collagen type I scaffolds.

Cells were seeded into 24 well plates in full serum culture medium and incubated for 24 hours to allow cell attachment. After 24 hours the culture medium was switched to low serum culture medium and incubated for another 24 hours. Forty-eight hours after initial seeding, the cells were treated with pro-form MMP-8 and incubated for 7 days. Initially 1nM and 10nM solutions of pro-form MMP-8 were used to treat MSCs in cells for 7 days with the medium changed every 3 days to evaluate cell viability in a collagenase (7). There were four groups for the pro-form MMP-8 treatments: 1 nM MMP-8, 1 nM vehicle control (PBS), 10 nM MMP-8, and 10 nM vehicle control (PBS). After 7 days the cells were collected and stored at -80°C. Then, 100 nM of pro-form MMPs 1, 2, 8 and 13 were used to treat MSCs for 3 days. There was a treatment group for each MMP and a vehicle control (phosphate buffered saline). After 3 days the cells were collected from the plates and stored at -80°C.

Scaffold Preparation

Scaffolds were cut into dog-bone shapes (typical of a uniaxial tensile test specimen) out of collagen type I sponges (DSM Biomaterials, Exton, PA). The scaffolds were sterilized by soaking in ethanol on a shaker table for 24 hours. After 24 hours of sterilization, the scaffolds were washed six times for 30 minutes in phosphate buffered saline (PBS) on the shaker table. The scaffolds were then stored in PBS at 4°C until ready to use.

Seeding wells for collagen scaffold culture were printed with acrylonitrile butadiene styrene (ABS) plastic using a 3-dimensional (3D) printer (Flashforge Inc.), treated with an acetone bath to seal pores, and sterilized in 70% ethanol before scaffold seeding. The scaffolds were incubated in full serum culture medium in a conical tube for 24 hours prior to seeding with MSCs. Scaffolds were placed into the 3D printed dog-bone shaped wells, seeded with MSCs in full serum culture medium to promote cell adhesion and attachment, and incubated for 24 hours. The culture medium was then changed to low serum culture medium, and the scaffolds were moved from the dog-bone shaped wells to culture wells and incubated for 24 additional hours. Two days after initial seeding with MSCs, the scaffolds were treated with pro-form MMPs 1, 2, 8, and 13 and incubated for 3 days. There was a

treatment group (n=2) and a vehicle control (n=2) for each pro-form MMP, except for the MMP-8 treatment group (n = 1). At day 3, the scaffolds were fixed in 10% formalin for 24 hours, rinsed with PBS, and stored at 4°C until they were imaged.

Matrix Metalloproteinases

Pro-form MMP-1, 2, 8, and 13 were purchased from R&D Systems and used to treat the cells and cell seeded scaffolds. MMP concentrations of 1 nM, 10 nM, and 100 nM were used to treat cells and scaffolds.

Imaging and Image Analysis

Scaffold imaging was done with an Olympus Fluoview 1000 Multiphoton Confocal Microscope with a 4x objective. To visualize the collagen structure, the scaffolds were imaged with second harmonic generation (SHG) imaging at a wavelength of 860 nm. Analysis of the SHG images was done by first editing the images with ImageJ (National Institute of Health, Bethesda, MD) to change the size, color, and image file type and to invert the color. The edited SHG images were then run through Fiberfit (Boise State University), an open-source software used to analyze the organization of the ECM structure of soft tissues (28).

Fiberfit

Fiberfit was originally used to quantify the alignment in the SHG images and obtain the “k value”, a measure of fiber alignment. However, our SHG images produced multi-modal histograms, which Fiberfit is not capable of accurately analyzing. Instead, Fiberfit was used to obtain histograms showing collagen fiber alignment angles versus frequency from the raw data, and an alternative post-processing method was used to assign an alignment value, k, to each peak on the histogram. Python was used for the image post processing. A “modified k value” was then calculated based on a weighted aggregation of filtered peaks extracted from a probability density function. Specific details on calculating the modified k value, including the developed code are in Appendix C on page 65.

Statistical Analysis

Python was used to run a one-way analysis of variance (ANOVA) and Tukey’s post hoc test between the modified k values of each control and treatment groups, with the MMP type as the single factor. The level of significance was set as $p < 0.05$. Data is reported as the mean +/- standard deviation.

Results

The initial experiment done with pro-form MMP-8 showed no apparent cytotoxicity to the MSCs, seen in Figure 2.1. Since there seemed to be no changes to cell viability or morphology at 1 nM or 10 nM of pro-form MMP-8, we treated MSCs with a higher concentration of pro-form MMP-1, 2, 8, and 13. There was some apparent cell death, but normal levels for low serum culture medium, in all groups including the control (based on some rounded cells), but no major morphology changes to the MSCs at 100 nM of pro-MMP-1, 2, 8, or 13 at 3 days (Figure 2.2). Thus, these MMPs were further explored in scaffolds. The scaffolds were then treated with 100 nM of pro-form MMPs 1, 2, 8, and 13. Scaffolds did not show any qualitative changes to collagen alignment, seen in Figure 2.3.

Fiber Alignment *(modified k)*

Pro-form MMP-1 ($p = 0.091$) and pro-form MMP-13 (0.118) treated groups had modified k values that trended higher compared to control groups but had no statistically significant differences.

Pro-form MMP-2 ($p = 0.279$) and Pro-form MMP-8 ($p = 0.417$) groups showed that the controls exhibited higher modified k values than the treated groups. These values are seen in Figure 2.4. Again, none of these values were statistically significant ($p < 0.05$).

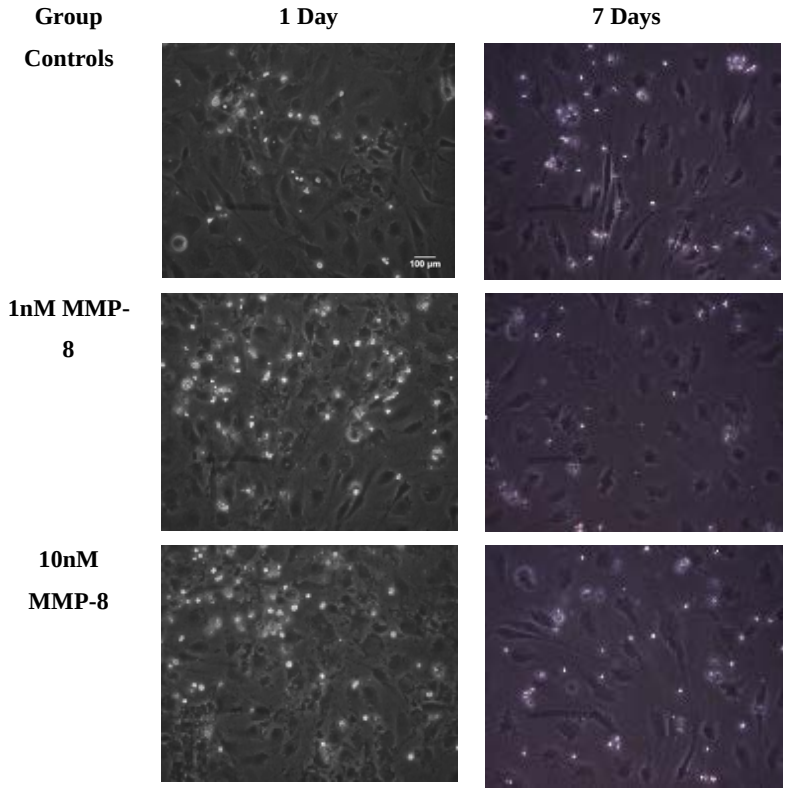

Figure 2.1: 1 nM and 10 nM of MMP-8 added to MSCs for 7days.

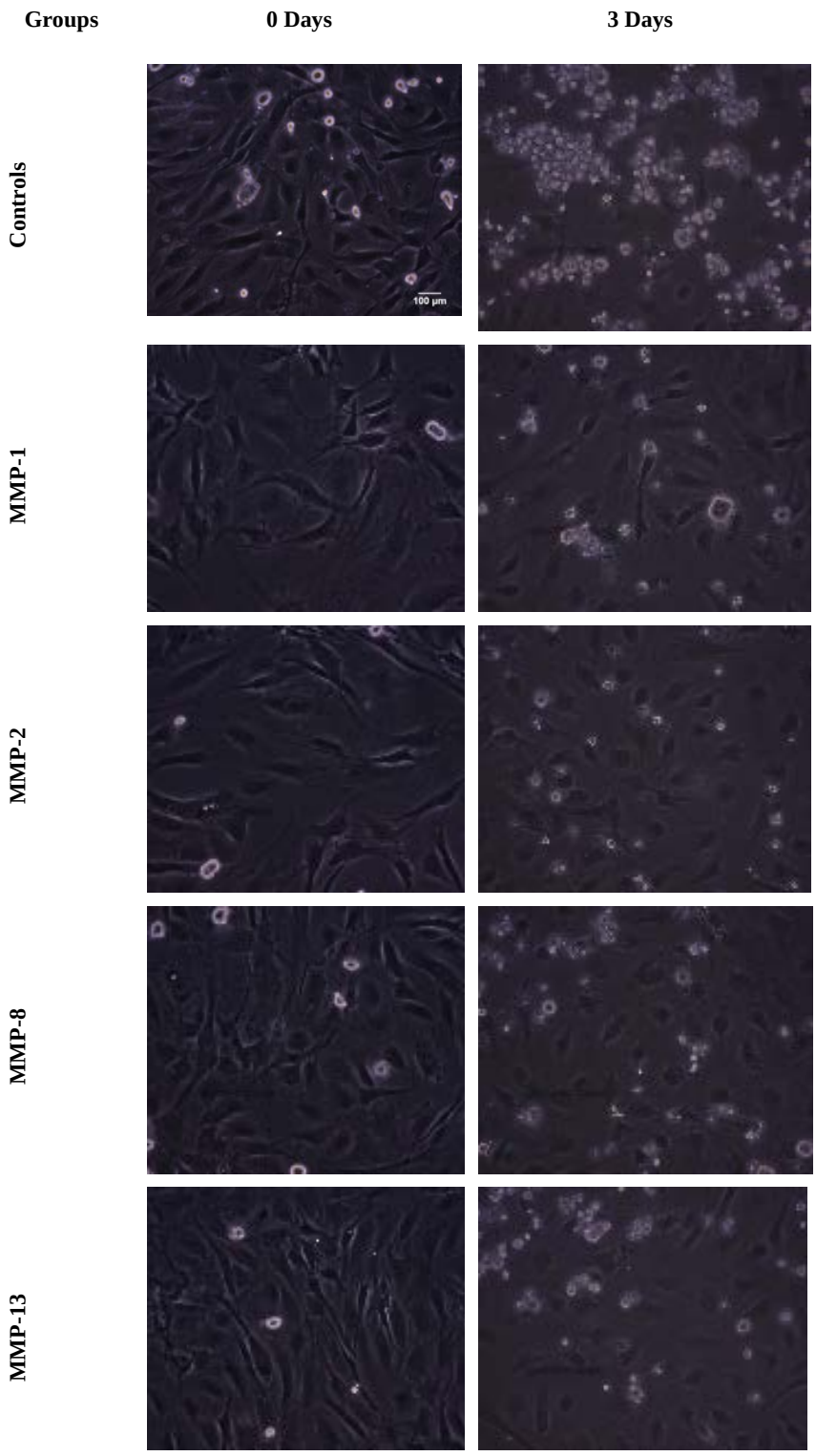

Figure 2.2: 100 nM of MMP-1, MMP-2, MMP-8, and MMP-13 added to MSCs for 3 days. Images taken with a 10x objective.

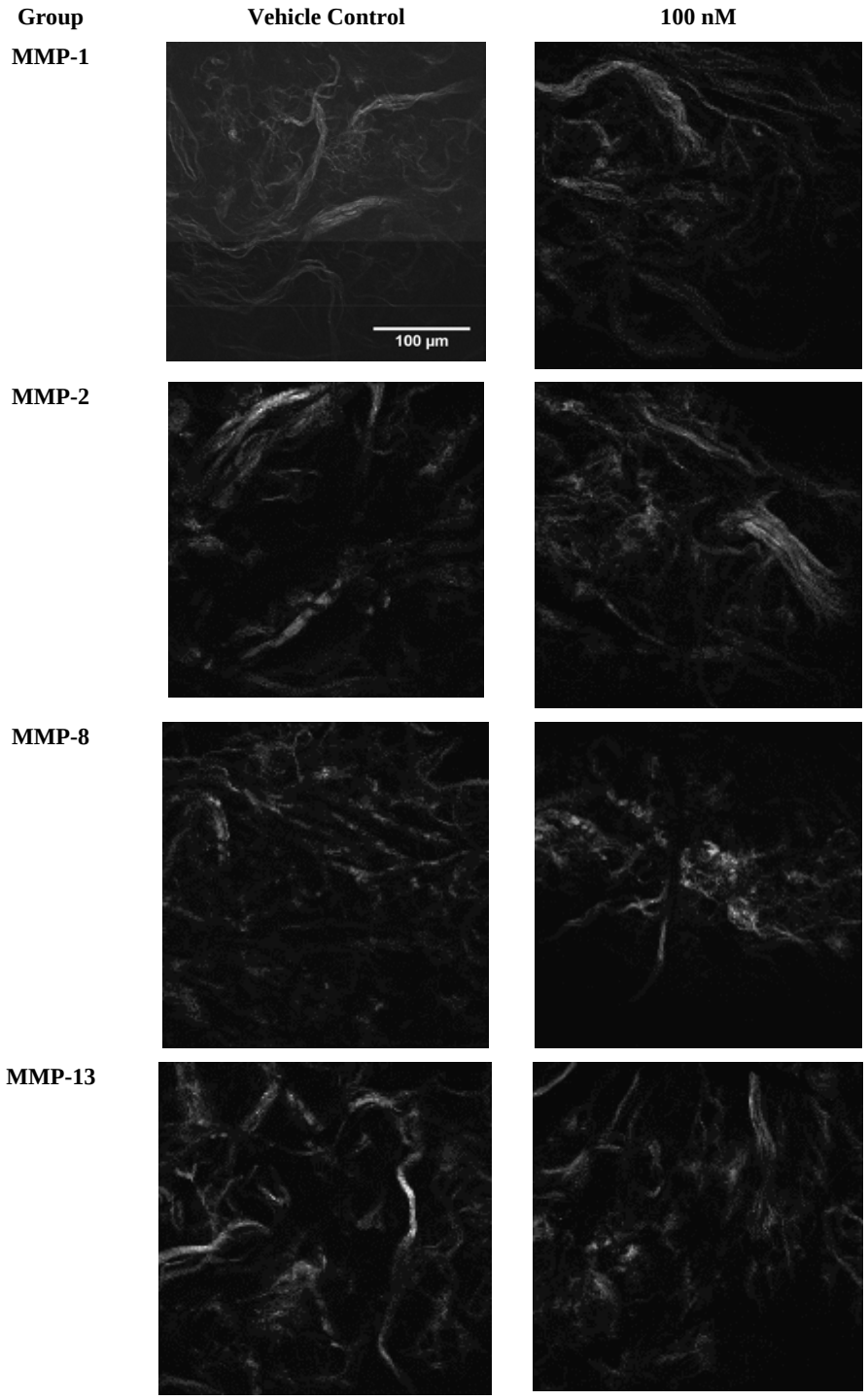

Figure 2.3: Scaffolds treated with 100 nM of MMPs or PBS (for the control groups) for 3 days. Images taken with a 4x objective.

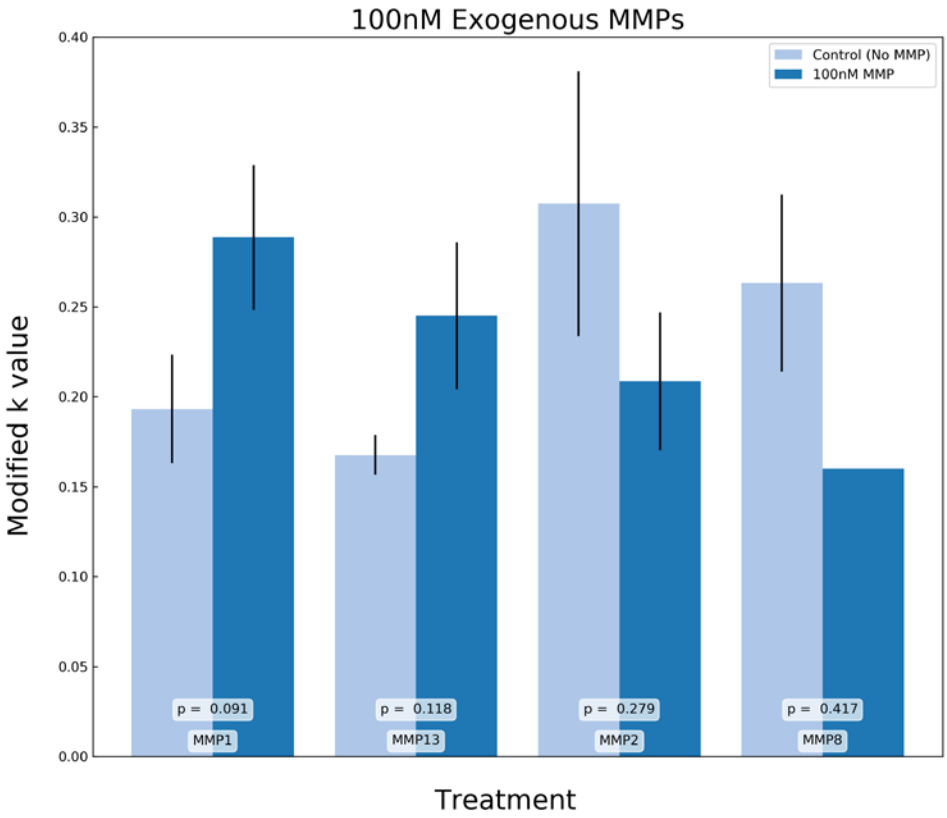

Figure 2.4: Collagen alignment (modified k values) for scaffolds treated with MMP-1, MMP-13, MMP-2, and MMP-8. Significance is determined by $p < 0.05$.

Discussion

MMP-8 was originally chosen for the initial test of 1 nM and 10 nM concentrations because it is a good representation of the collagenases, and collagen type I is its known substrate. Observation of the effects of varying concentrations of pro-form MMP-8 on MSCs was conducted to give a general idea of how MSCs in low serum cell culture may respond, at the very least, compared to other collagenases for a longer 7-day timepoint.

Scaffolds treated with 100 nM of each MMP did not show any visible changes in the collagen fiber structure between the controls and treatment groups. While MSCs have mechanisms to activate pro-form MMPs (e.g., through MT-MMPs), it is possible that the MSCs may be inhibiting the exogenous MMPs through the production of tissue inhibitors of MMPs (TIMPs) (19, 29). It is also possible that the MSCs may be inhibiting the exogenous MMPs that we added to the culture (29). This makes sense based on the Fiberfit data in Figure 2.4. While there were minor changes in the collagen fiber alignment (i.e., modified k value), none of these changes were statistically significant. MMPs are such potent enzymes that we expected to see a more consistent collagen degradation of the unaligned collagen fibers using pro-form MMPs. While this was true in some groups, it was not seen in others. However, because MMPs are very potent and activation may be tightly regulated by MSCs, it is

possible that in our system the MSCs did not activate the MMPs. MMPs degrading collagen unchecked could be problematic and damaging, suggesting that the addition of regulatory factors (such as MMP activators) may be necessary (27). We concluded that exogenous MMPs may require activation to have noticeable effects on collagen.

Another factor that may be affecting the collagen is cellular behavior. Since the MSCs were not visualized in these scaffolds for this pilot project, there could have been cellular behavior unaccounted for. It is possible that there were no significant observed changes to the collagen due to other unknown changes to the seeded MSCs, or secretion of TIMPs. Therefore, the next step was to treat the collagen scaffolds and MSCs with the active form of these MMPs and to stain the MSCs to understand if there are any potential cellular impacts (Chapter 3).

Chapter 3: Impact of Activated Matrix Metalloproteinases on Tenogenically Differentiating Mesenchymal Stem Cells and Collagen Type I Scaffolds

Introduction

Matrix metalloproteinases (MMPs) are important enzymes for tissue remodeling. They have been shown to be the main proteinases that degrade and breakdown collagen, one of the most abundant structural proteins in the body (8, 9). Tendon is composed of 70-80% collagen (at its dry weight), and much of the physical support in tendon tissue is provided by this collagen (1). When tendon is damaged, it is often the underlying collagen that is affected, and healing involves depositing disorganized collagen in the form of scar (1). The current treatment involves surgery, and reinjury rates post-surgical intervention are high (1). Since tendon injuries and tendinopathies are common, a functional tendon replacement is needed.

One potential treatment method for directing collagen fiber alignment in collagen-based scaffolds is the application of MMPs. Based on our data presented in Chapter 2, MMPs may need to be activated to impact the collagen fiber network in our engineered scaffolds. Since unchecked MMP activity can be harmful, expression in healthy tissue is normally low and expression of active MMPs is higher during embryonic development and healing (27). This may be why activation is necessary. *In vivo*, activation is often done by other MMPs, such as membrane tethered MMPs (MT-MMPs), and other enzymes, such as trypsin (8, 18). *Ex vivo*, different compounds may be added to the MMPs to trigger activation. Compounds such as 4-Aminophenylmercuric acetate (APMA) and serine proteinases have been used for MMP activation (20).

The effects of active MMPs in tendon tissue with the addition of tenogenic growth factors, such as transforming growth factor beta 2 (TGFβ2), and mesenchymal stem cells (MSCs) on disorganized collagen are unknown. The release of active MMPs into tissue may not lead to remodeling by itself, and other factors are often required for guiding remodeling, such as the ones mentioned above (7).

In Chapter 2, where the effects of pro-form MMP-1, 2, 8, and 13 on collagen type I scaffolds were evaluated, there was no significant change to the alignment of the disorganized collagen network in the scaffolds. This may be due to the tight regulation of MMPs. Since unregulated MMPs can cause tissue damage, it is possible that there was little degradation of the collagen due to the enzymes not being activated. Therefore, the objective of this study was to determine how activated MMPs impacted tenogenically differentiating MSCs both in 2-dimensional (2D) standard cell cultures and in collagen type I scaffolds. In this experiment, the effects of activated MMP-1, 2, 8, and 13 are observed in MSCs that were tenogenically induced using TGFβ2. MSC growth may be impacted by

MMPs, so the cells were observed in standard 2D culture before treating MSC-seeded collagen type I scaffolds with active MMPs (7).

Materials and Methods

Cell Culture

Mouse C3H10T1/2 MSCs were purchased from American Type Culture Collection (ATCC, Manassas VA), expanded using our standard cell culture protocols and growth medium (Dulbecco's Modified Eagle's Medium (DMEM), 10% fetal bovine serum (FBS), and 1% Penicillin/ Streptomycin), and passaged every three to four days. MSCs were seeded at 5,000 cells/cm^2 into 24-well plates and 500,000 MSCs per scaffold were seeded into collagen type I scaffolds.

Table 3.1: Treatment Conditions for plated cells and scaffolds.

1 nM Active MMP-1 + TGFβ2	1 nM Active MMP-1 Control (H20) + TGFβ2
10 nM Active MMP-1 + TGFβ2	10 nM Active MMP-1 Control (H20) + TGFβ2
1 nM Active MMP-2 + TGFβ2	1 nM Active MMP-2 Control (H20) + TGFβ2
10 nM Active MMP-2 + TGFβ2	10 nM Active MMP-2 Control (H20) + TGFβ2
1 nM Active MMP-8 + TGFβ2	1 nM Active MMP-8 Control (PBS) + TGFβ2
10 nM Active MMP-8 + TGFβ2	10 nM Active MMP-8 Control (PBS) + TGFβ2
1 nM Active MMP-13 + TGFβ2	1 nM Active MMP-13 Control (PBS) + TGFβ2
10 nM Active MMP-13 + TGFβ2	10 nM Active MMP-13 Control (PBS) + TGFβ2

Cells were seeded into 24 well plates in full serum culture medium and incubated for 24 hours to allow cell attachment. After 24 hours the culture medium was switched to low serum culture medium and incubated for another 24 hours. Forty-eight hours after initial seeding, the cells were treated with active MMPs 1, 2, 8, and 13 and incubated for either 3 or 7 days. Initially, 1 nM and 10 nM concentrations of MMP 1, 2, 8, and 13 were used to treat MSCs in cells for 7 days with the medium changed every 3 days (9). Treatment groups are shown in Table 3.1.

Scaffold Preparation

Scaffolds were cut into dog-bone shapes out of collagen type I sponges (DSM Biomaterials, Exton, PA). The scaffolds were sterilized by soaking in ethanol on a shaker table for 24 hours. After 24 hours of sterilization, the scaffolds were washed six times for 30 minutes in phosphate buffered saline (PBS) on the shaker table. The scaffolds were then stored in PBS at 4°C until ready to use. Seeding wells for collagen scaffold culture were 3D printed with acrylonitrile butadiene styrene (ABS) plastic, treated with an acetone bath to seal pores, and sterilized in 70% ethanol before scaffold seeding. The scaffolds were incubated in full serum culture medium in a conical tube for 24 hours prior to seeding with MSCs. Scaffolds were placed into 3D printed dog bone shaped wells with cells to promote cell adhesion and attachment and incubated for 24 hours. The culture medium was then changed to low

serum culture medium, and the scaffolds were moved from the dog bone shaped wells to culture wells and incubated for 24 additional hours.

Forty-eight hours after initial seeding, the cells were treated with 50 ng/mL TGFβ2 to induce tenogenesis in MSCs and active MMP- 1, 2, 8, or 13 and then incubated for either 3 or 7 days (3). The medium was changed on day 3 for the 7-day timepoints. Conditions for each group are shown below in Table 3.1. At either 3 or 7-days, the cover slips and scaffolds were fixed with 10% formalin for 24 hours at 4°C, then washed with phosphate buffered saline (PBS) and stored in PBS at 4°C.

Matrix Metalloproteinases and Activation

MMP-1, 2, 8, and 13 were used to treat the MSCs and MSC seeded scaffolds. Experimentation was initially conducted to determine how to activate the MMPs using 4-Aminophenylmercuric acetate (APMA) and Trypsin TPCK (7). 1 mM APMA was used but proved to be cytotoxic (20). As a result, Trypsin TPCK was used at 0.1 mg/mL for MMP-1, 8, and 13, and 100 ug/mL for MMP-2 (20). An activation protocol from Chondrex (Redmond, WA) was used and activation was determined by spectrophotometry (20). MMP-1, MMP-2 (Peprotech, Rocky Hill, NJ), and MMP-13 (Chondrex, Redmond, WA) were purchased in their activated form. MMP-8 could not be purchased in its active form and was purchased in its pro-form from Chondrex (Redmond, WA). MMP-8 was activated by treating with trypsin TPCK at 0.1 mg/mL for 1 hour at 37°C using the protocol from the *Chondrex Collagenase Assay Kit* (20, 31).

Scaffold and Cover Slip Staining

The scaffolds were stained with 4,6-Diamidino-2- phenylindole (DAPI) and FITC-Phalloidin to visualize the cell nuclei and actin cytoskeleton, respectively. The staining procedure requires two, five-minute washes in 0.1% Triton-X. A 1% BSA-Triton-X solution was made and included the DAPI and Phalloidin stain at 1:2000 and 1:100 respectively. Each scaffold was placed in 250 µL of stain for one hour, with the scaffolds being flipped over after 30 minutes on one side. The stained scaffolds were stored at 4°C in conical tubes filled with PBS and wrapped in aluminum foil. The cover slips were also stained using DAPI and FITC-Phalloidin, but for one hour and then mounted onto slides.

Imaging and Image Analysis

Scaffold imaging was done on an Olympus Fluoview 1000 Multiphoton Confocal Microscope. The scaffolds were imaged (20x objective) with DAPI and Phalloidin staining to observe any changes to cell morphology, and with second harmonic generation imaging (4x objective) to observe changes to collagen structure. Cover slips were imaged with a Nikon Spinning Disk Confocal Microscope (20x

objective). Analysis of the SHG images was done by first editing the images in ImageJ (image editing software from the National Institute of Health) to change the size, color, and image file type and to invert the colors. The edited SHG images were then run through a modified version of Fiberfit (Boise State University) to analyze the collagen alignment (28).

Fiberfit

Fiberfit was originally going to be used for image analysis, to quantify the alignment in the SHG images. However, our SHG images produced multi-modal histograms, which Fiberfit is not capable of accurately analyzing. Instead, Fiberfit was used to obtain histograms showing collagen fiber alignment angles versus frequency from the raw data, and a different post processing method was used to assign an alignment value, k, to each peak on the histogram. Python was used for the image post processing. The k value was calculated based on a weighted aggregation of filtered peaks extracted from a probability density function. Specific details on calculating the modified k value, including the developed code, are in Appendix C on page 65.

Statistical Analysis

Prism was used to run a two-way analysis of variance (ANOVA) and Tukey's post hoc test between the modified k values of each control and treatment groups. The level of significance was set as $p < 0.05$. Data is reported as the mean +/- standard deviation.

Results

Initially, activation of pro-form MMPs was attempted with 1 mM AMPA, as previously described (20). However, the APMA appeared cytotoxic with significant cell death occurring within 24 hours. Therefore, we explored a less cytotoxic MMP activation compound, Trypsin TPCK. Trypsin TPCK was used with the *Collagenase Activation* procedure from Chondrex to activate MMP-8 (20, 31). MMP-1, MMP-2 and MMP-13 were purchased in their activated forms. Concentrations of 1 nM and 10 nM MMP were selected to treat the tenogenically differentiating MSCs on the scaffolds and cover slips, each for 3 and 7 days. Figure 3.5, Figure 3.6, Figure 3.7, and Figure 3.8 show the SHG images of the scaffolds. Cell morphology for each time point and concentration are shown in bright field images in Figure 3.1, Figure 3.2, Figure 3.3, Figure 3.4, and collagen fibers in scaffolds are shown in Figure 3.5, Figure 3.6, Figure 3.7, Figure 3.8. DAPI and Phalloidin stained MSCs on the cover slips are shown in Figure A.1, Figure A.2, Figure A.3, and Figure A.4.

The brightfield images of MSCs in Figure 3.1, Figure 3.2, Figure 3.3, Figure 3.4 were viable and exhibited normal cell morphology. There were no obvious visible changes between any of the groups in the stained images or the SHG images. The tenogenically differentiating MSCs had normal

morphology and were viable. Collagen fiber degradation in the SHG images varied between groups but did not show any qualitative trends or visible degradation. Quantitative data for the scaffolds was generated by analyzing the modified collagen fiber alignment value (modified k) with Fiberfit and our developed post processing method (shown in Appendix C) (28).

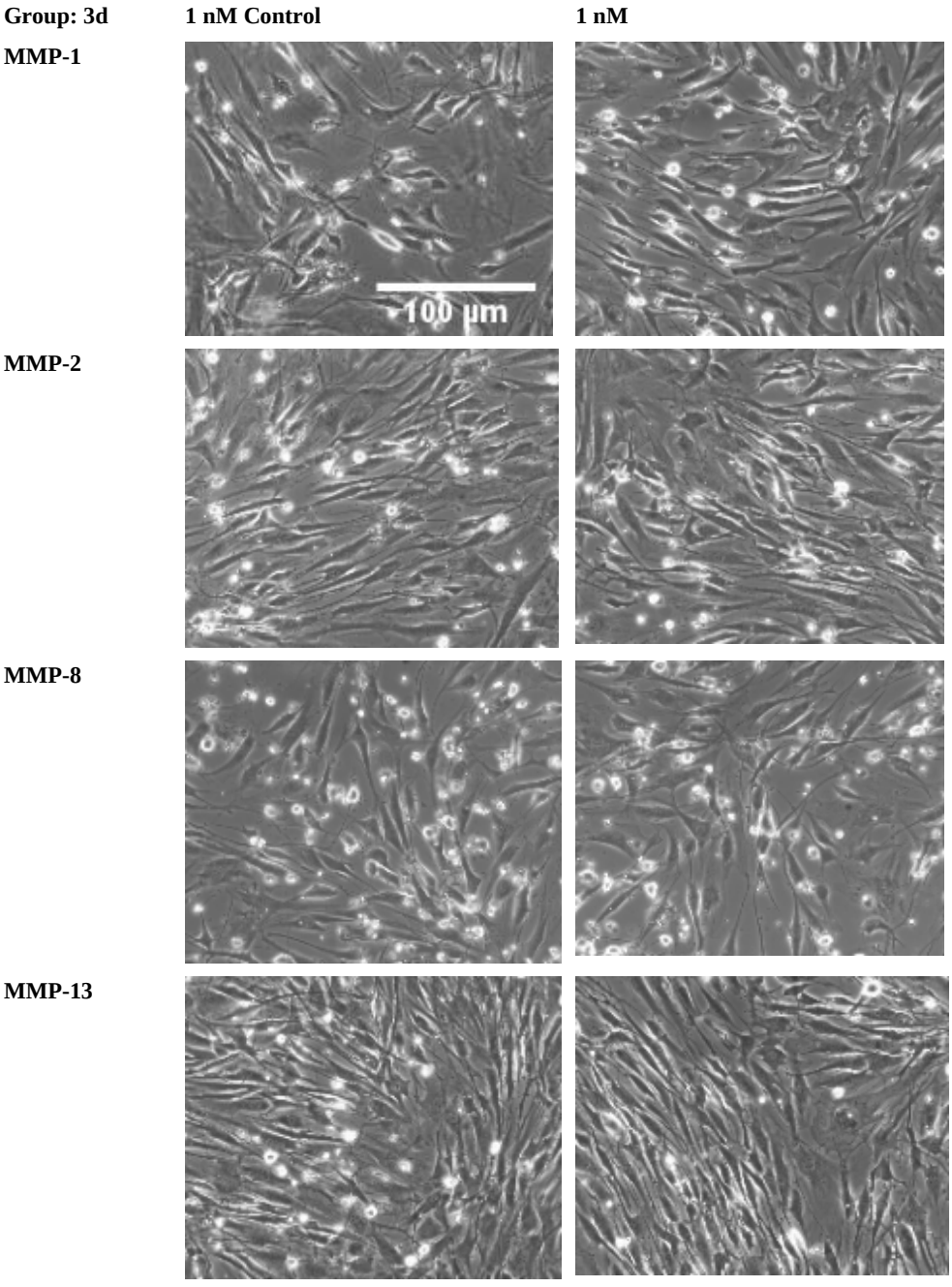

Figure 3.1: Images (10x objective) of cover slips in 24 well plates and treated with TGFβ2 and 1 nM of active MMP-1, 2, 8, or 13 for 3 days.

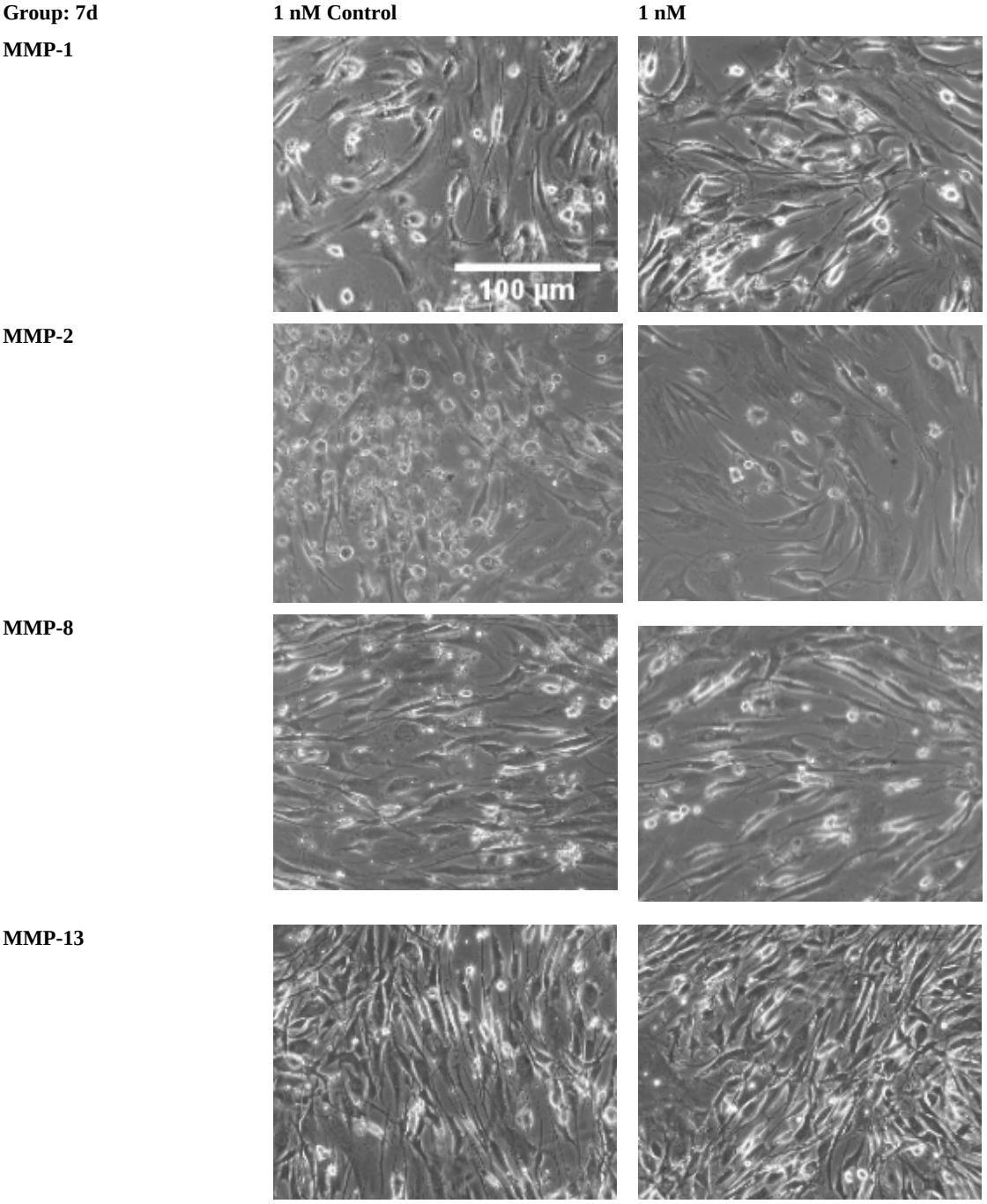

Figure 3.2: Images (10x objective) of cover slips in 24 well plates and treated with TGFβ2 and 1 nM of MMP-1, 2, 8, or 13 for 7 days.

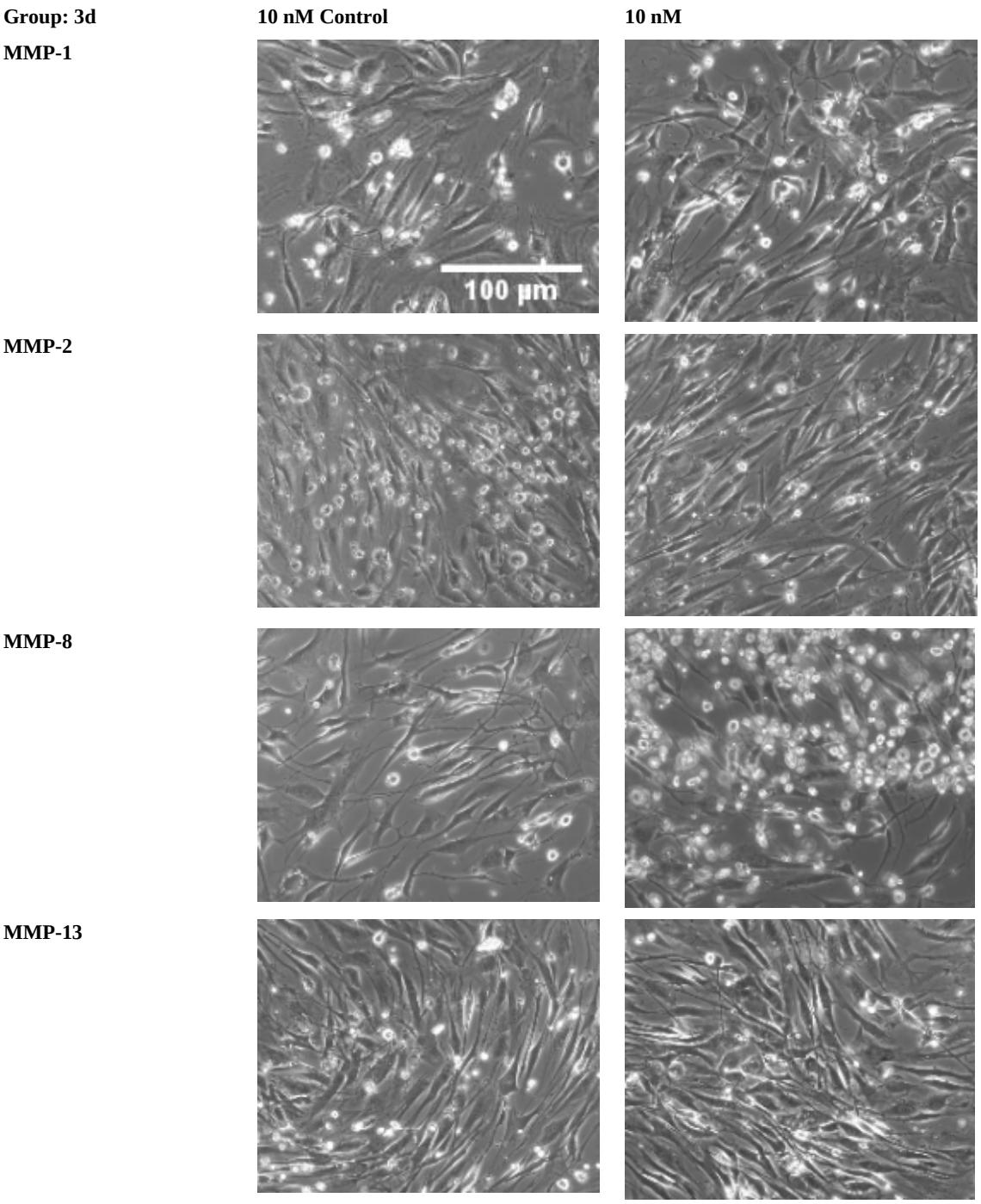

Figure 3.3: Images (10x objective) of cover slips in 24 well plates and treated with TGFβ2 and 10 nM of MMP-1, 2, 8, or 13 for 3 days.

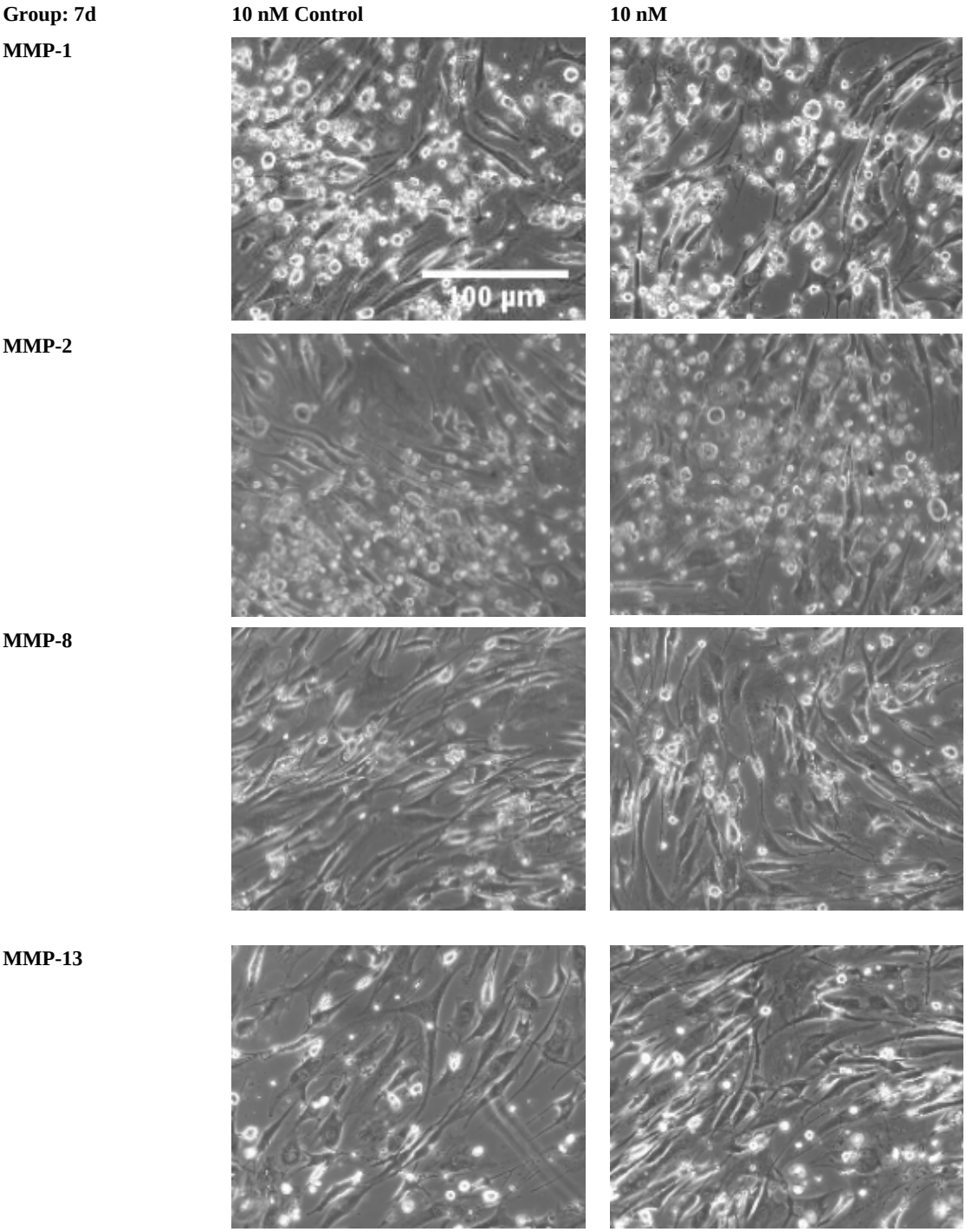

Figure 3.4: Images (10x objective) of cover slips in 24 well plates and treated with TGFβ2 and 10 nM of MMP-1, 2, 8, or 13 for 7 days.

Group: 3d	Imaging	1 nM Control	1 nM
MMP-1	**DAPI & Phalloidin**	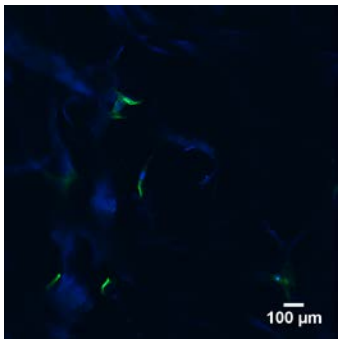	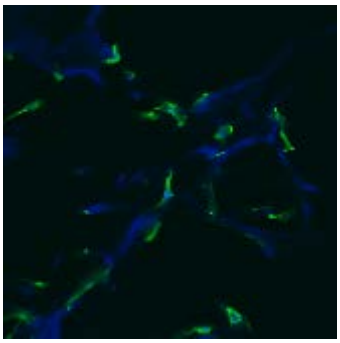
	SHG	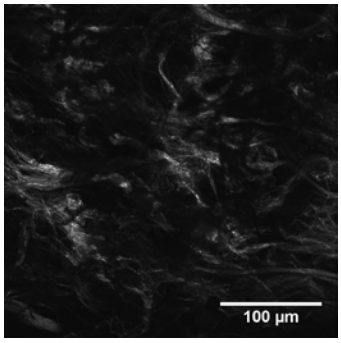	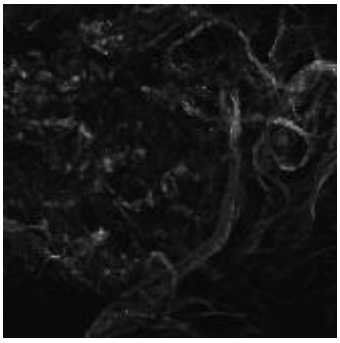
MMP-2	**DAPI & Phalloidin**	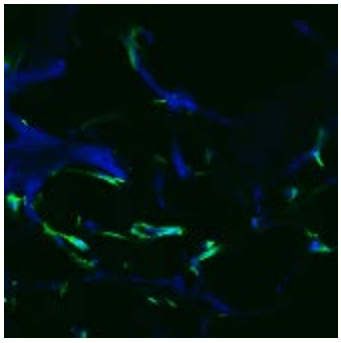	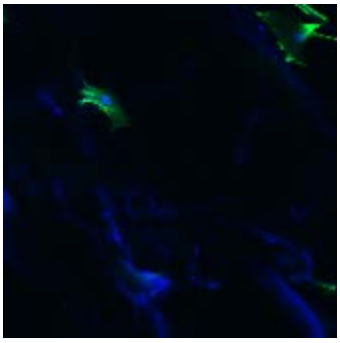
	SHG	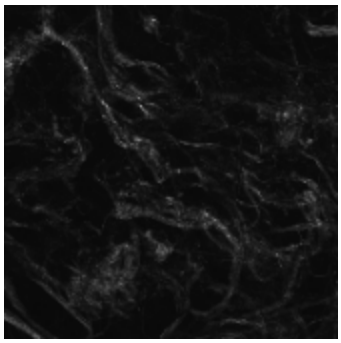	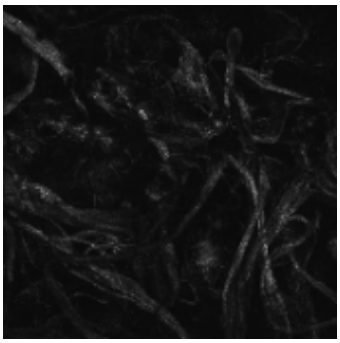

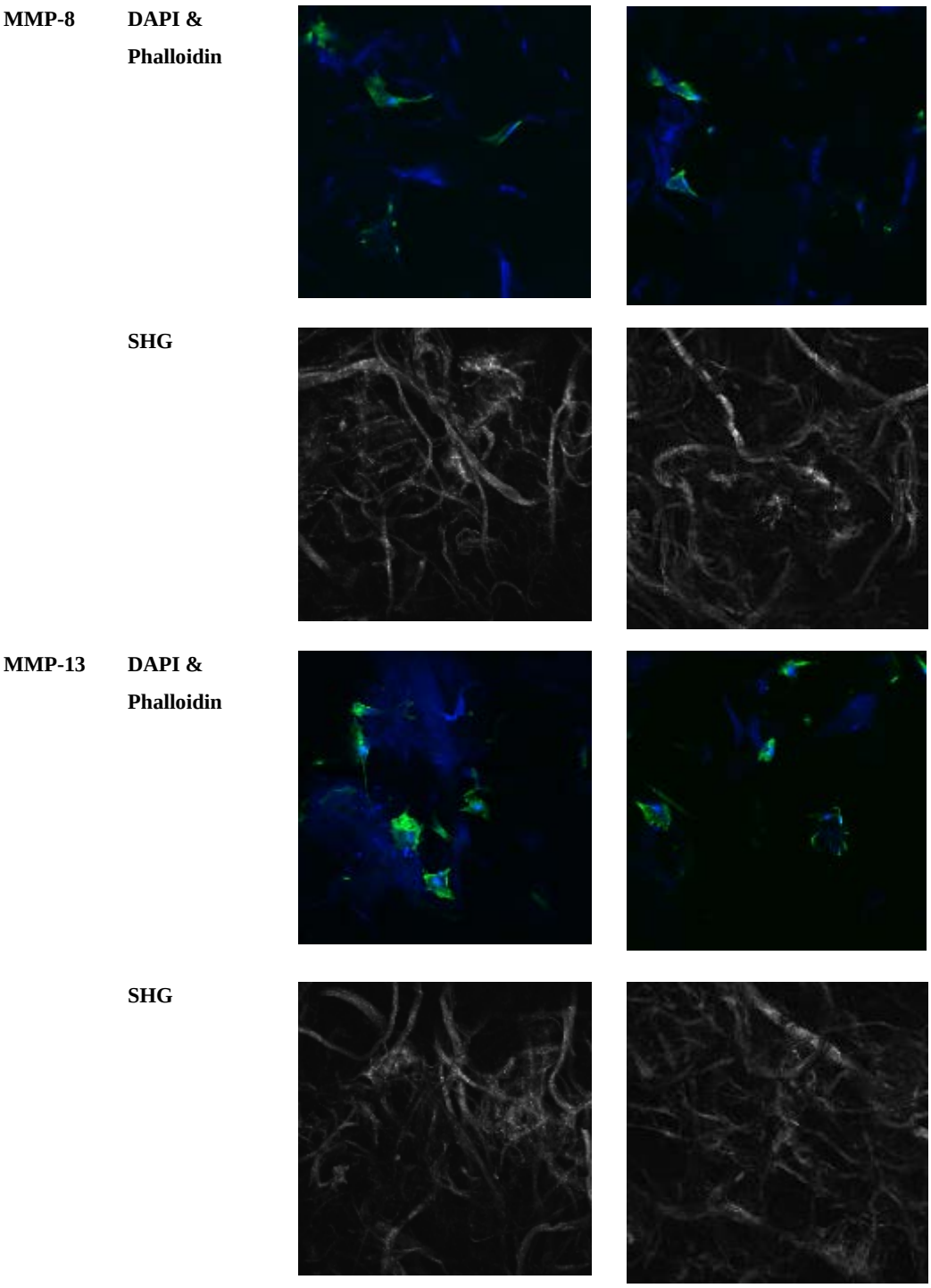

Figure 3.5: Images of scaffolds treated with TGFβ2 and 1nM of MMP-1, 2, 8, or 13 for 3 days. Green and blue images are the MSCs stained with DAPI and Phalloidin (20x objective). The black and white images are SHG images showing the collagen fibers in each scaffold (4x objective).

Group: 7d	Imaging	1 nM Control	1 nM
MMP-1	DAPI & Phalloidin	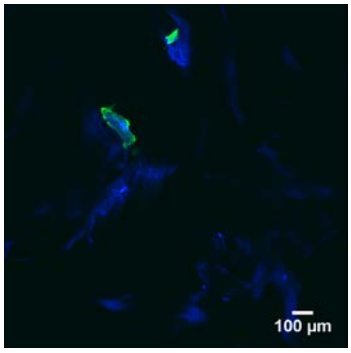	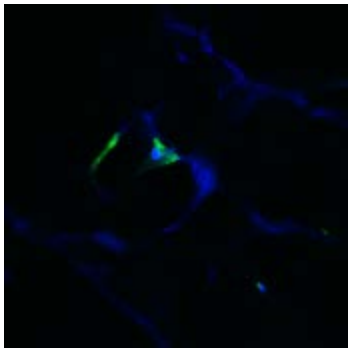
	SHG	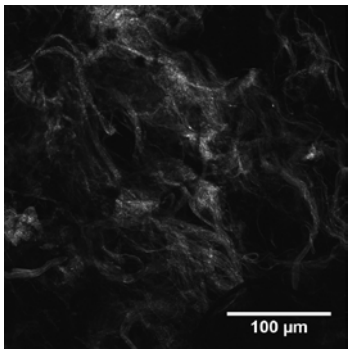	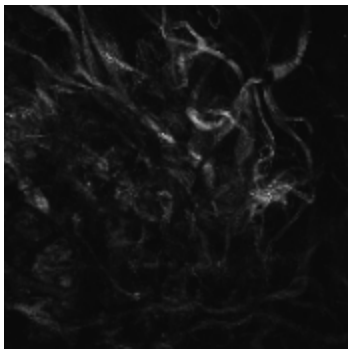
MMP-2	DAPI & Phalloidin	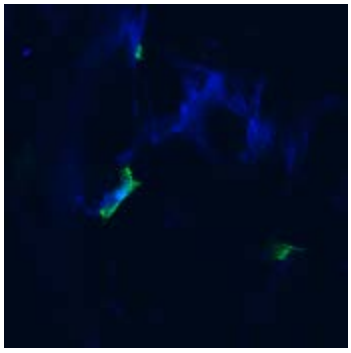	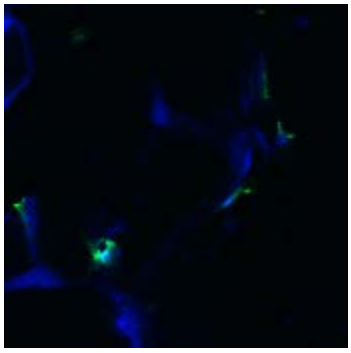
	SHG	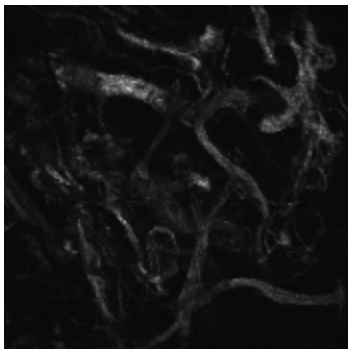	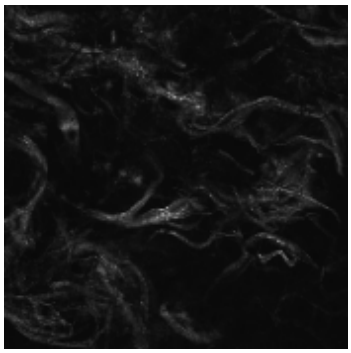

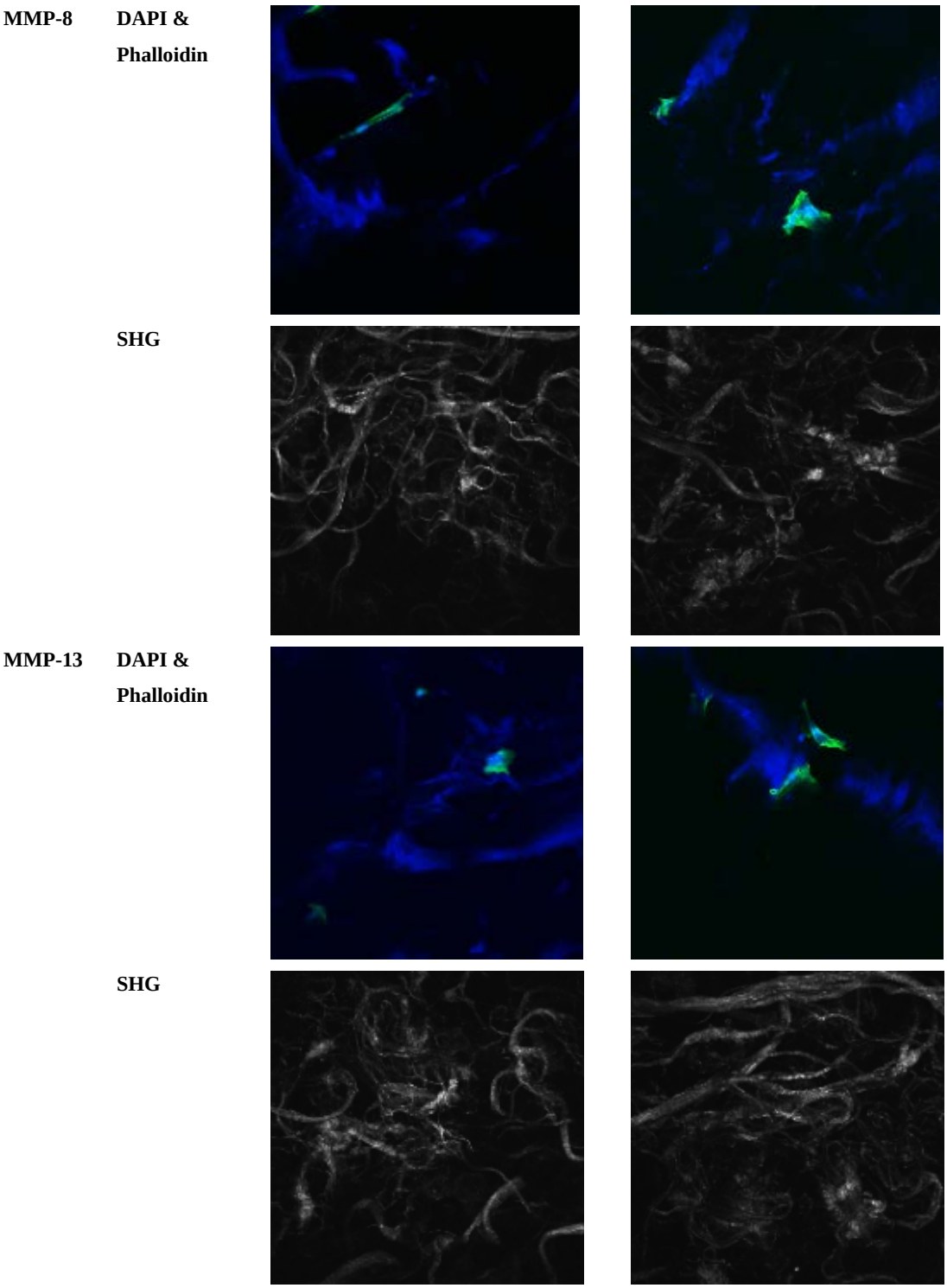

Figure 3.6: Images of scaffolds treated with TGFβ2 and 1nM of MMP-1, 2, 8, or 13 for 7 days. Green and blue images are the MSCs stained with DAPI and Phalloidin (20x objective). The black and white images are SHG images showing the collagen fibers in each scaffold (4x objective).

Group: 3d	Imaging	10 nM Control	10 nM
MMP-1	DAPI & Phalloidin	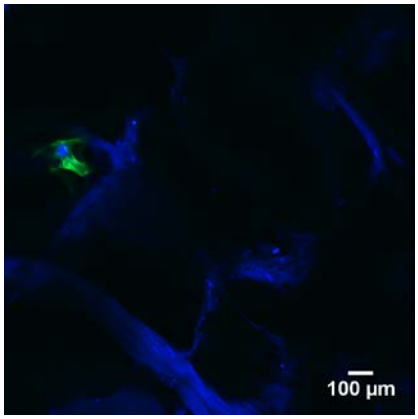	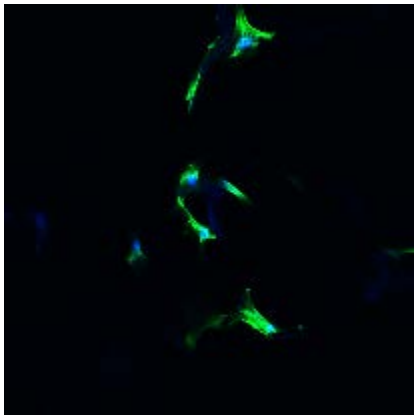
	SHG	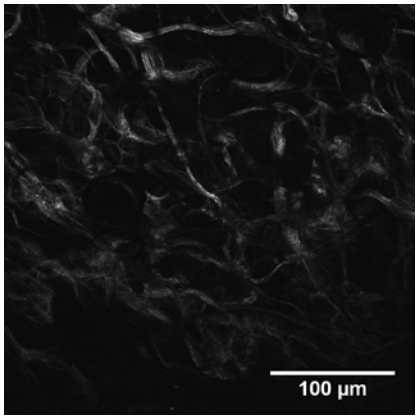	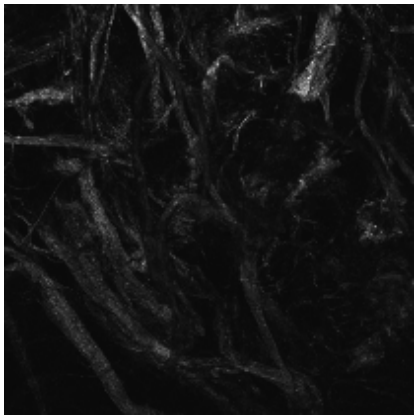
MMP-2	DAPI & Phalloidin	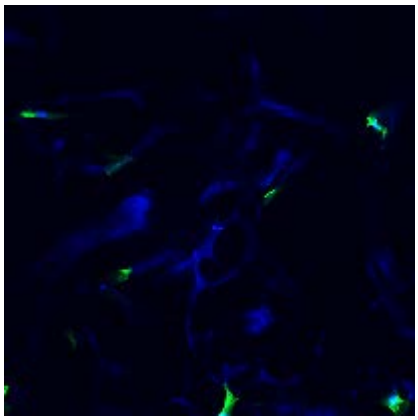	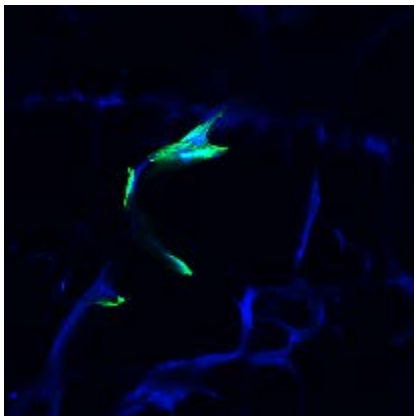

	SHG	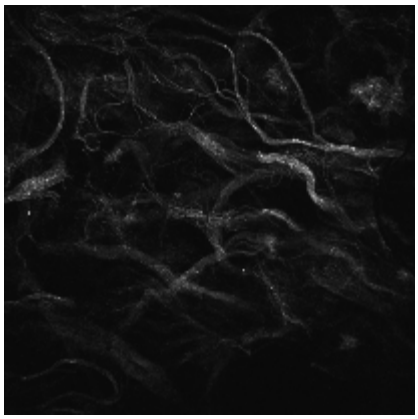	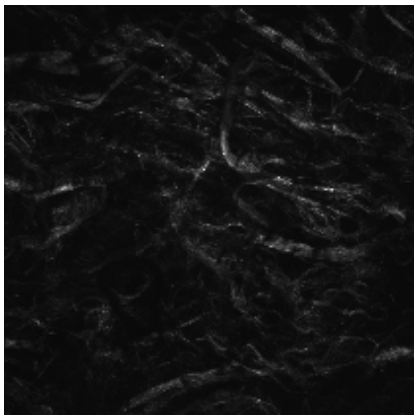
MMP-8	**DAPI & Phalloidin**	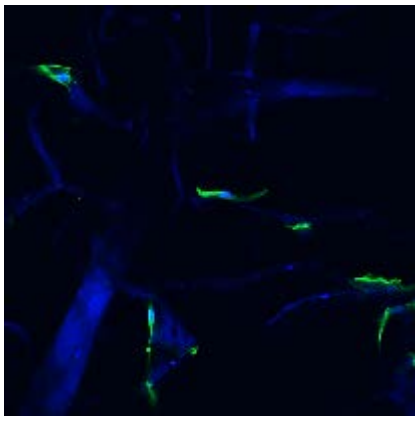	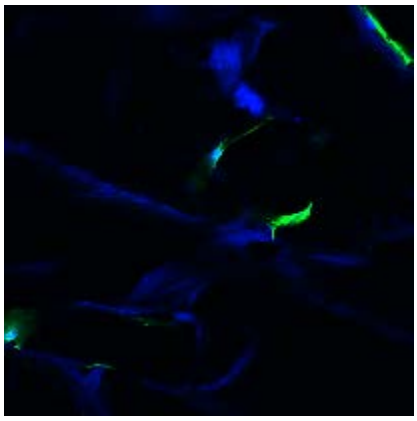
	SHG	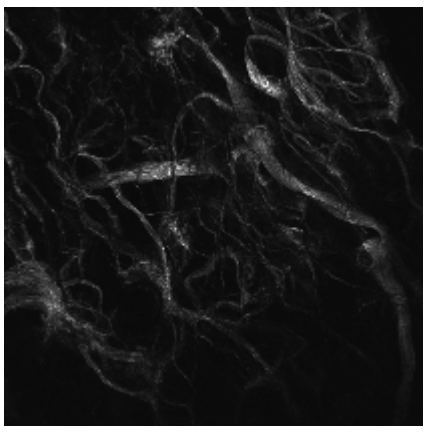	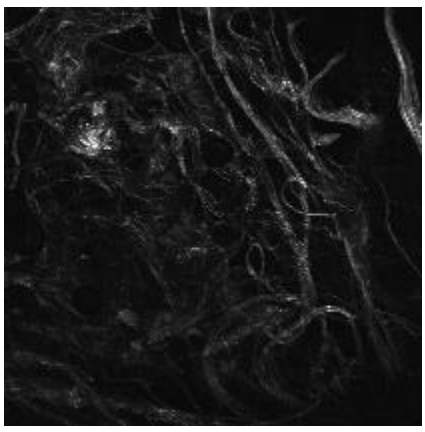
MMP-13	**DAPI & Phalloidin**	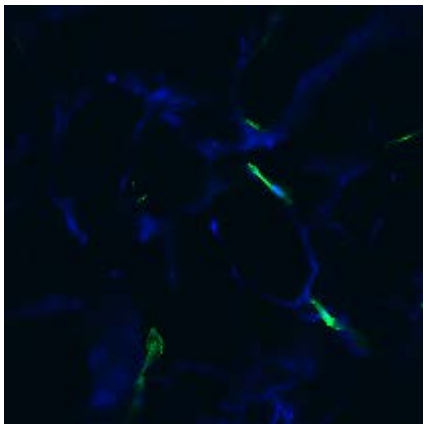	

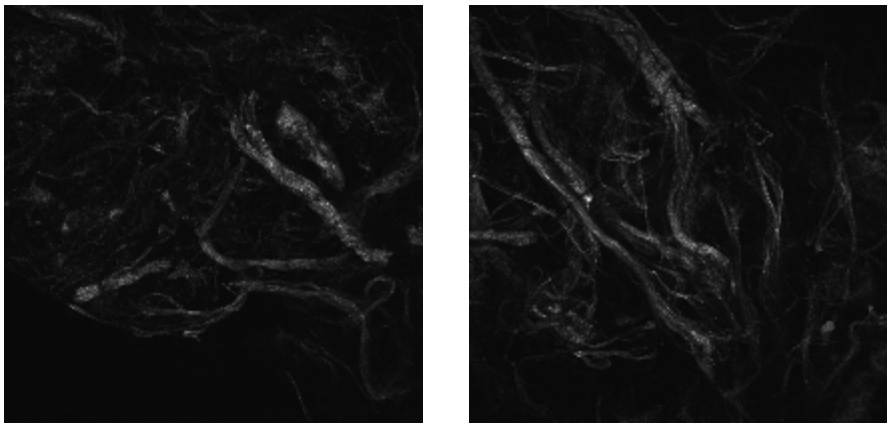

Figure 3.7: Images of scaffolds treated with TGFβ2 and 10 nM of active MMP-1, 2, 8 for 3 days. Green and blue images are the MSCs stained with DAPI and Phalloidin (20x objective). The black and white images are SHG images showing the collagen fibers in each scaffold (4x objective).

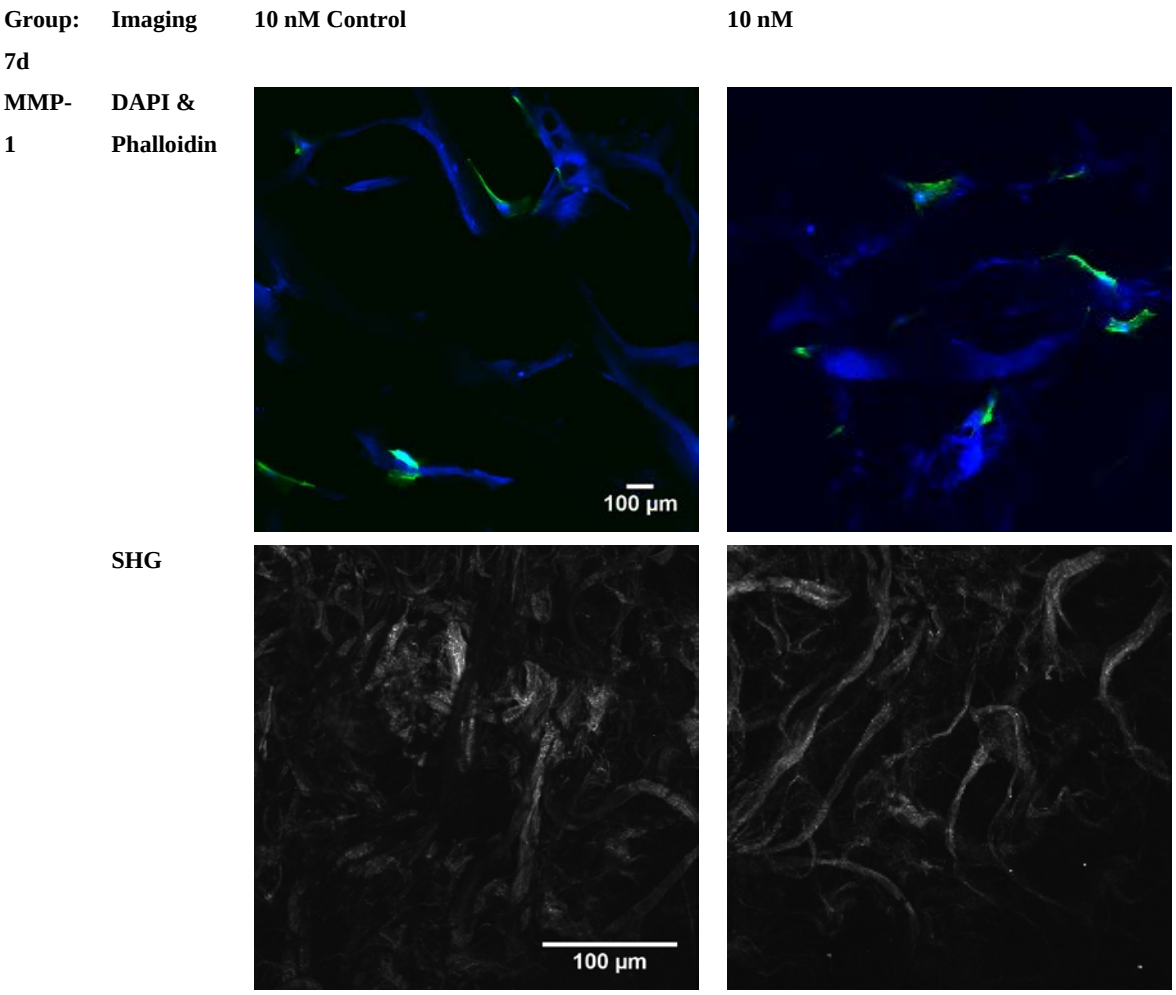

MMP-2	**DAPI & Phalloidin**	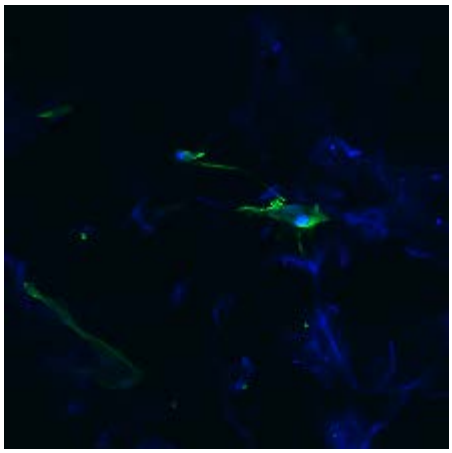	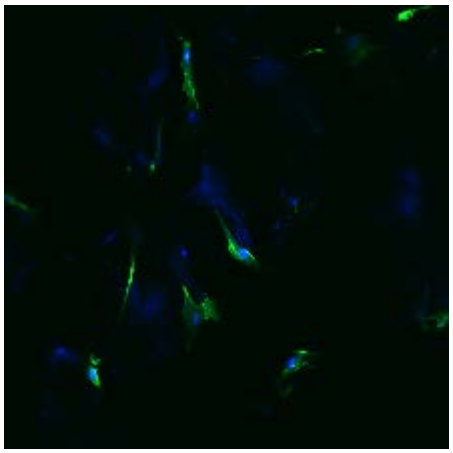
	SHG	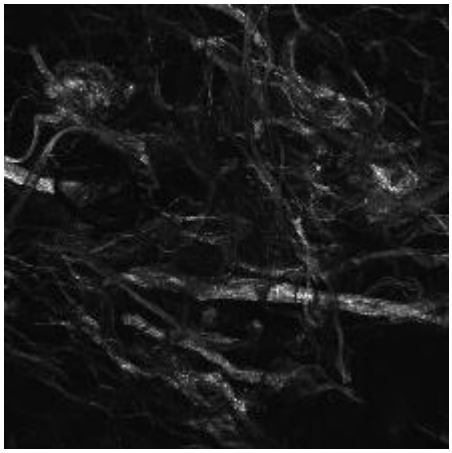	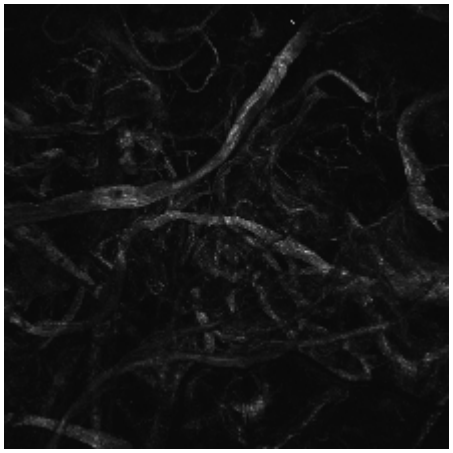
MMP-8	**DAPI & Phalloidin**	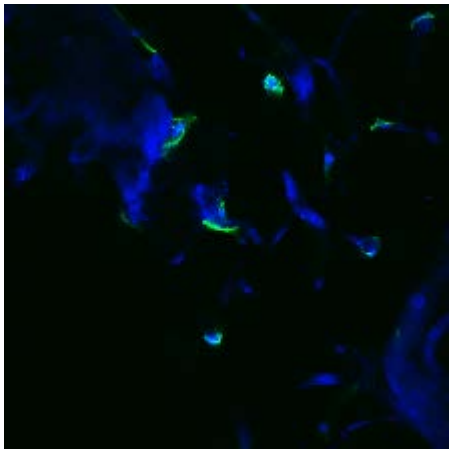	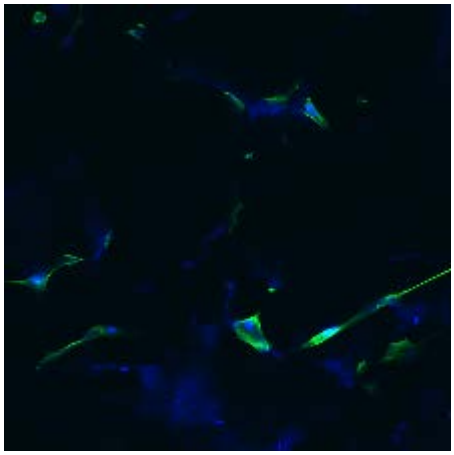

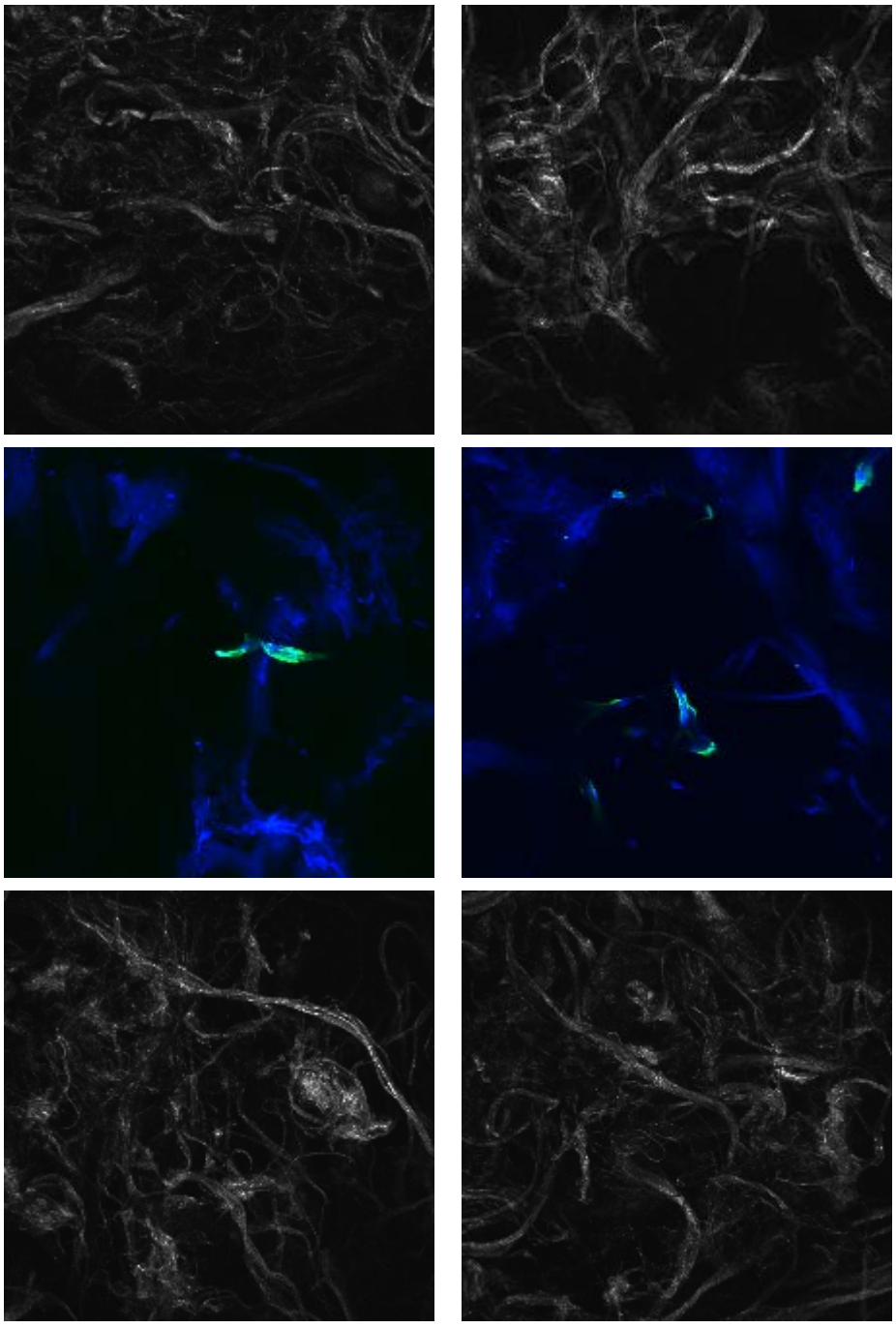

Figure 3.8: Images of scaffolds treated with TGFβ2 and 10 nM of active MMP-1, 2, 8 for 7 days. Green and blue images are the MSCs stained with DAPI and Phalloidin (20x objective). The black and white images are SHG images showing the collagen fibers in each scaffold (4x objective).

Fiber alignment (modified k)

Modified k values are shown in bar plots in Figure 3.9. Each treatment group was compared to its control group and compared against the different time points and concentrations. No statistically significant differences were found between any groups ($p < 0.05$), and no obvious trends were seen. P values for all comparisons of groups can be seen in Table A.1.

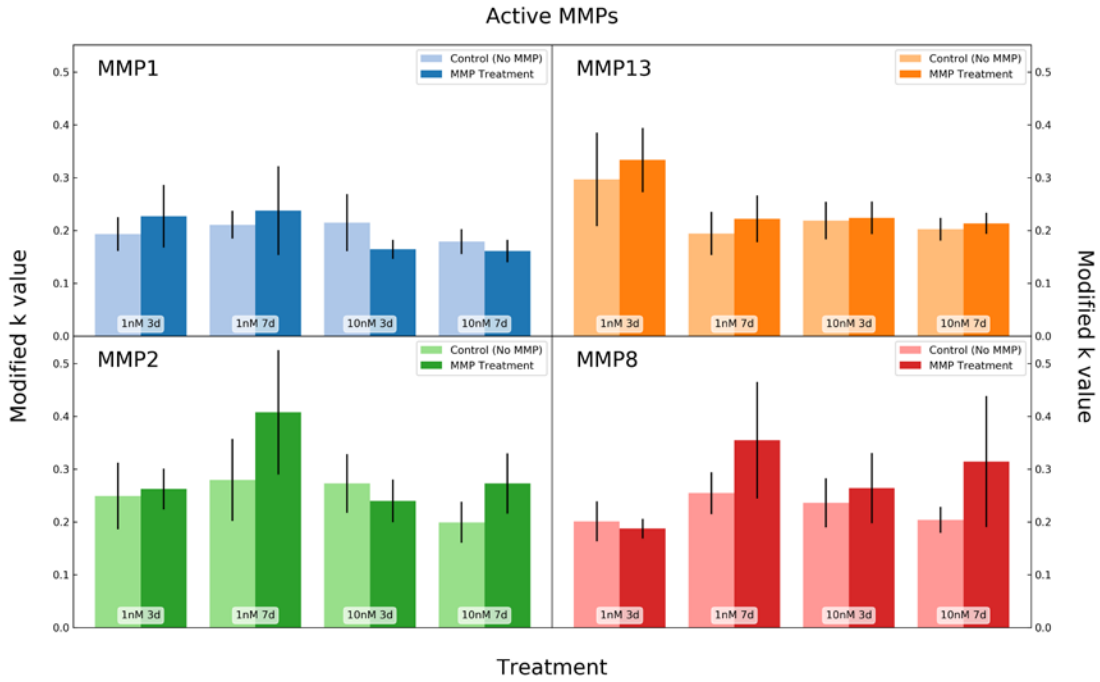

Figure 3.9: Modified k values (fiber alignment) of the collagen scaffolds treated with either 1 nM or 10 nM of MMP-1, 2, 8, or 13 for 3 or 7 days. Top left is MMP-1. Bottom left is MMP-2. Bottom right is MMP-8. Top right is MMP-13.

Discussion

There were no obvious visible changes to the tenogenically differentiating MSCs with active MMP treatments. The MSCs appeared viable in all groups, showing no cytotoxicity from the active MMPs or Trypsin TPCK across concentrations and time points.

The modified k values showed no statistically significant differences between treatment and control groups, time points, or concentrations. A limitation is the small sample sizes (n=3) and the high cost of the activated MMPs makes it difficult to use higher sample sizes. Furthermore, as discussed in Chapter 2, MMPs are highly regulated due to their potentially harmful properties when unchecked, so it is possible that the tenogenically differentiating MSCs produced TIMPs to limit MMP activity (29). To test this hypothesis, it would be worth analyzing the collagen structure treated with active MMPs, but not seeded with MSCs. However, when the same collagen type I scaffolds were treated with

bacterial collagenase and mechanical loading, they demonstrated higher alignment in the treated groups versus the controls (34), suggesting the collagen fibers can be modified by enzymes. Additionally, the collagen type I scaffolds have also been shown to degrade in medium for extended periods of time without cells (33). Taken together, exploring how tenogenically differentiating MSCs regulate active MMPs would be interesting in future studies.

It has been found that the release of MMPs and tissue inhibitors of MMPs (TIMPs) alone into collagen will not cause organized collagen fiber remodeling (7). This suggests that other cues may be needed for the MMPs to fully exhibit their selective degradative properties, such as mechanical stimulation (e.g., strain protection) (7, 25, 52). Mechanical stimulation can reduce enzymatic cleavage rates by stabilizing the collagen fibers, allowing new organized collagen to be deposited along the axis of strain and the unorganized collagen to be degraded (7). It is likely that some combination of these factors (MSCs, TGFβ2, MMPs, and mechanical stimulation) will increase organized collagen formation. This was explored in Chapter 4.

Chapter 4: Impact of Activated Matrix Metalloproteinases and Tensile Strain on Tenogenically Differentiating Mesenchymal Stem Cells and Collagen Type I Scaffolds

Introduction

Mechanical loading is an important aspect of musculoskeletal development, particularly for tendons (21). Tendons require mechanical stimulation to maintain their mechanical properties and for normal development (2, 10). When tendons are injured, their mechanical function is limited. They also have limited ability to heal, and tendon injuries often result in chronic or acute tendinopathy (1). Developing a tissue engineered tendon construct using MSCs, biochemical signals, and scaffolds will be important for the future of tendon injuries. In Chapter 2 and Chapter 3 we explored the effects of MMPs and TGFβ2 on MSC seeded collagen scaffolds. We found that it is likely these biochemical signals combined with mechanical stimulation are needed to increase organized collagen formation.

In a study exploring decellularized pericardium, biaxial and uniaxial strain dependent collagen degradation changed the collagen fiber alignment to match the direction of the strain (25). This suggests that the collagen fibers align where there is little degradation, and the aligned fibers are protected from degradation, matching the *Strain Protection Theory* (7, 25, 52). However, there were limitations in this case such as using bacterial collagenase rather than MMPs, and importantly for tissue engineering, this was not explored with cells (25, 52). In other studies, it was shown that MMP-8 in combination with mechanical strain preserved collagen fibrils (7). This may be due to the fact that mechanical loading causes collagen molecules to pack together, and this packing decreases their suceptibility to enzymatic cleavage (25). When the collagen aligns, the strained fibers are protected from enzymatic degradation and the other fibers are degraded by the MMPs (7, 52). This leads to collagen matrix remodeling (7). Matrix remodeling is important for tendon tissue engineering and tendon formation.

The objective of this study was to explore how activated MMPs in combination with mechanical strain impacted tissue formation in engineered tendon tissues. The combination of MSCs with mechanical loading, MMPs, and TGFβ2 in collagen scaffolds has not been studied for tendon tissue engineering applications. These experiments were conducted to observe how the application of 5% tensile strain and active MMP-1, 2, 8, and 13 impact the collagen alignment in collagen type I scaffolds seeded with tenogenically differentiating MSCs. We predicted that the application of strain to scaffolds would protect the mechanically loaded collagen fibers from MMP degradation and result in higher collagen fiber alignment. We also predicted that the mechanical properties of collagen type I scaffolds treated with active MMP-2 and 5% strain would be improved.

Materials and Methods

Cell Culture

Mouse C3H10T1/2 MSCs were purchased from American Type Culture Collection (ATCC, Manassas VA), expanded using our standard cell culture protocols and growth medium (Dulbecco's Modified Eagle's Medium (DMEM), 10% fetal bovine serum (FBS), and 1% Penicillin/ Streptomycin), and passaged every three to four days. MSCs were seeded into collagen type I scaffolds.

Table 4.1: Treatment Conditions

Treatment Groups 5% Strain	Control Groups 0% Strain
10 nM Active MMP-1 & TGFβ2	10 nM Active MMP-1 & TGFβ2
10 nM Active MMP-2 & TGFβ2	10 nM Active MMP-2 & TGFβ2
10 nM Active MMP-8 & TGFβ2	10 nM Active MMP-8 & TGFβ2
10 nM Active MMP-13 & TGFβ2	10 nM Active MMP-13 & TGFβ2
50 ng/mL TGFβ2 only	50 ng/mL TGFβ2 only

Scaffold Preparation

Scaffolds were cut into dog-bone shapes out of collagen type I sponges (DSM Biomaterials, Exton, PA). The scaffolds were sterilized by soaking in ethanol on a shaker table for 24 hours. After 24 hours of sterilization, the scaffolds were washed six times for 30 minutes in phosphate buffered saline (PBS) on the shaker table. The scaffolds were then stored in PBS at 4°C until ready to use.

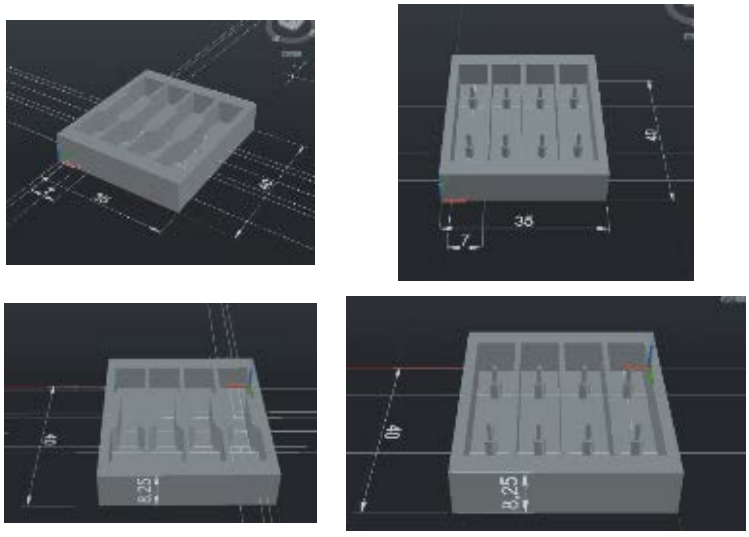

Figure 4.1: Updated design of scaffold seeding wells. Dog-bone shaped wells for cell seeding and new dimensions are shown on the left. Modified culture wells and dimensions are shown on the right.

Seeding wells for collagen scaffold culture were redesigned to be able to hold a greater volume, seen in Figure 4.1. The pegs inside were also modified to be able to better hold the scaffolds in place. The differences between the new and old seeding wells are seen in Figure 4.2. The seeding wells were 3D printed with acrylonitrile butadiene styrene (ABS) plastic, treated with an acetone bath to seal pores, and sterilized in 70% ethanol before scaffold seeding. The scaffolds were incubated in full serum culture medium in a conical tube for 24 hours prior to seeding with MSCs. Scaffolds were placed into 3D printed dog

bone shaped wells and seeded with cells at 20,000 cells/cm^2 to promote cell adhesion and attachment and incubated for 24 hours (26).

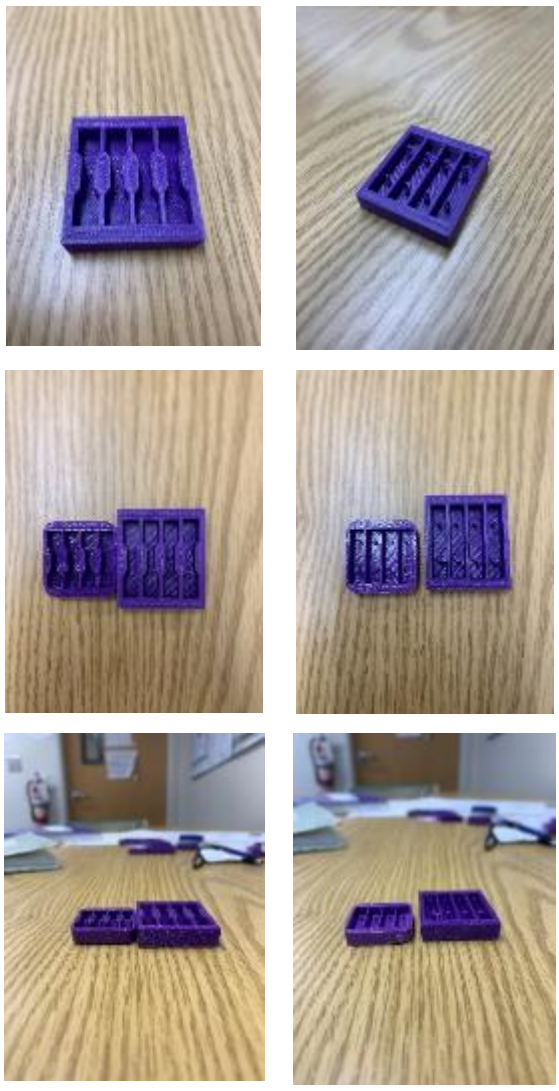

Figure 4.2: Dog-bone shaped seeding wells and culture wells. Images above show the comparisons between the new and old designs.

After 24 hours, the culture medium was changed to low serum culture medium, the scaffolds were moved from the dog bone shaped wells to culture wells, 5% strain was applied, and scaffolds were incubated for 24 additional hours. Forty-eight hours after initial seeding, the cells were treated with 50 ng/mL TGFβ2 to induce tenogenesis in MSCs (3) and 10 nM of active MMP- 1, 2, 8, or 13 then incubated for 7 days. There were six treatment groups, shown in Table 4.1. The medium was changed on day 3. At 7 days, the cover slips and scaffolds were fixed with 10% formalin for 24 hours at 4°C, then washed with phosphate buffered saline (PBS) and stored in PBS at 4°C.

Static Strain Applied to MSC-seeded Scaffolds in Culture

Each scaffold was measured with calipers and cut to 29 millimeters. Strain was applied by measuring each scaffold and pushing it onto the pegs 6.9 mm in from each end to achieve 5% strain. Control groups were pushed onto the pegs in a relaxed position, so they were not undergoing any strain. Cell-seeded scaffolds were then incubated for 7 days.

Uniaxial Mechanical Testing

Mechanical testing was done after 7 days of culture by placing scaffolds in a custom-made bioreactor and pulling until failure. The bioreactor was connected to a custom LabView program to control the load-frame and collect the force (using a 500 g load cell) and displacement data. The scaffolds were preconditioned by undergoing 10 cycles of 10% strain and pulled at a displacement rate of 0.1 mm/s. The scaffolds were then pulled to failure at a rate of 0.1 mm/s.

Matrix Metalloproteinases and Activation

MMP-1 and MMP-2 were purchased in their activated form (Peprotech, Rocky Hill, NJ). MMP-13 was purchased from Chondrex (Redmond, WA). MMP-8 could not be purchased in its active form and was purchased in its pro-form from Chondrex (Redmond, WA). MMP-8 was activated by treating with trypsin TPCK at 0.1 mg/mL for 1 hour at 37°C using the protocol from the *Collagenase Assay Kit* (20, 31).

Scaffold Staining

The scaffolds were stained with 4,6-Diamidino-2- phenylindole (DAPI) and FITC-Phalloidin to visualize the cell nuclei and actin cytoskeleton, respectively. The staining procedure requires two five-minute washes in 0.1% Triton-X. A 1% BSA-Triton-X solution was made and included the DAPI and Phalloidin stain at 1:2000 and 1:100 respectively. Each scaffold was placed in 250 µL of stain for one hour, with the scaffolds being flipped over after 30 minutes on one side. The stained scaffolds were stored at 4°C in conical tubes filled with PBS and wrapped in aluminum foil. The cover slips were also stained using DAPI and FITC-Phalloidin, but for one hour and then mounted onto slides.

Imaging and Image Analysis

Scaffold imaging was done on an Olympus Fluoview 1000 Multiphoton Confocal Microscope. The scaffolds were imaged with DAPI and phalloidin stain (20x objective) to observe any changes to cell morphology, and with second harmonic generation imaging (4x objective) to observe changes to collagen structure. Analysis of the SHG images was done by first editing the images in ImageJ (download from the National Institute of Health) to change the size, color, and image file type and to invert the colors. The edited SHG images were then run through Fiberfit (downloaded from Boise State University) to analyze the collagen structure (28).

Fiberfit

Fiberfit was originally going to be used for image analysis, to quantify the alignment in the SHG images. However, our SHG images produced multi-modal histograms, which Fiberfit is not capable of accurately analyzing. Instead, Fiberfit was used to obtain histograms showing collagen fiber alignment angles versus frequency from the raw data, and a different post processing method was used to assign an alignment value, k, to each peak on the histogram. Python was used for the image post processing. The k value was calculated based on a weighted aggregation of filtered peaks extracted from a probability density function. Specific details on calculating the modified k value, including the developed code, are in Appendix C (page 65).

Statistical Analysis

Python was used to run an unpaired, two tailed t-test between the modified k values of each control and treatment groups. The level of significance was set as $p < 0.05$. Data is reported as the mean +/- standard deviation.

Results

Representative SHG images and stained MSCs are shown in Figure 4.3. There were no dramatic qualitative changes to the morphology of the tenogenically differentiating MSCs based on the Phalloidin and DAPI staining between the strained (5% tensile strain) and the unstrained (0% tensile strain) groups. However, taken together, the strain groups appeared have MSCs with more elongated actin filaments that ran along the collagen fibers (see the active MMP-2 treated group as an example). The TGFβ2-only treated groups appeared to have larger aggregates of relatively less elongated cells compared to the MMP-treated groups. Qualitatively, the collagen structure visualized with SHG did not appear to have differences between strained or controls groups. After analyzing the images with Fiberfit and our developed method for image post-processing, we see that all scaffolds treated with MMPs and 5% strain have a higher modified k value than the control groups treated with 0% strain (Figure 4.4). However, none of the changes between groups were statistically significant ($p < 0.05$). Based on the increased MSC elongation seen in the Phalloidin staining in the MMP-2 groups (Figure 4.3) and the prior work showing high MMP-2 levels during embryonic tendon development (23), MMP-2 treatments were explored to observe the mechanical properties of the scaffolds.

A uniaxial tensile pull-to-failure test was conducted on scaffolds (n=3) that were strained and treated with 10 nM MMP-2 + 5% strain, 10 nM MMP-2 + 0% strain, and groups that were not treated with MMP-2 (TGFβ2-only) for 7 days. Fiberfit was used to produce histograms that show the alignment angles of the collagen fibers in the SHG images (Figure 4.5.) From these histograms, localized alignment appears to be occurring (though the difference in alignment (i.e., modified k value) between groups was not statistically significant). Though not quantified, MMP- and strain-treated groups appeared to have more prominent localized alignment (i.e., peaks at specific intervals between angles), compared to the control groups. For example, the peaks of localized alignment were occurring at various intervals relative to each other that were approximately 45°, 90° or 180° from the previous peak. A similar trend was seen for all MMP+5% strain groups.

From tensile testing, the stiffness, elastic modulus, stress, strain, and cross-sectional area were measured, and can be seen in Figure 4.6. No statistically significant differences were detected between the mechanical properties of MMP-2 + 5% strain, MMP-2 + 0% strain, TGFβ2 only + 5% strain, or the TGFβ2 only + 0% strain groups (p-values seen in Table B.1).

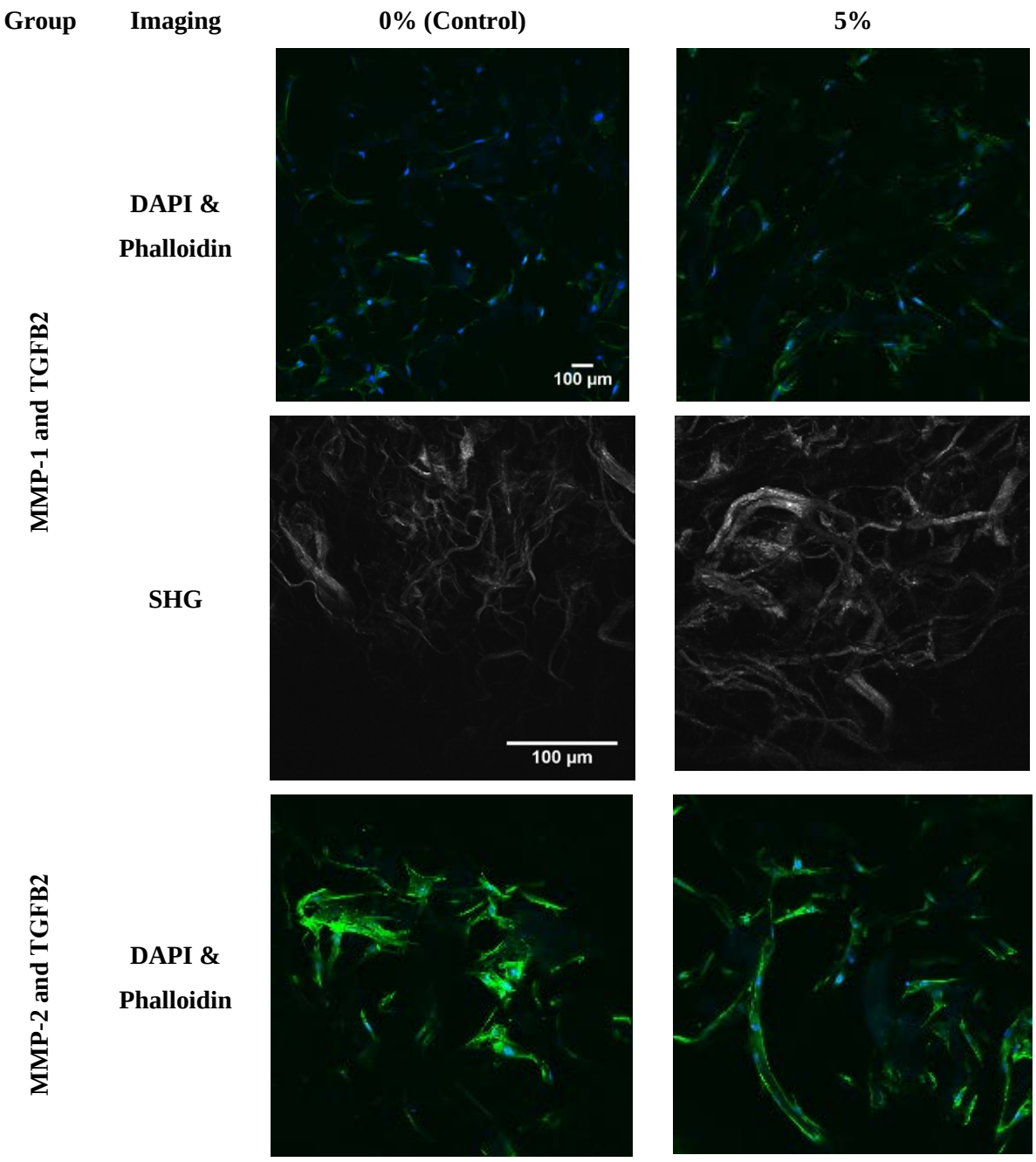
Group
Imaging
0% (Control)
5%
MMP-1 and TGFB2
DAPI & Phalloidin
100 µm
SHG
100 µm
MMP-2 and TGFB2
DAPI & Phalloidin

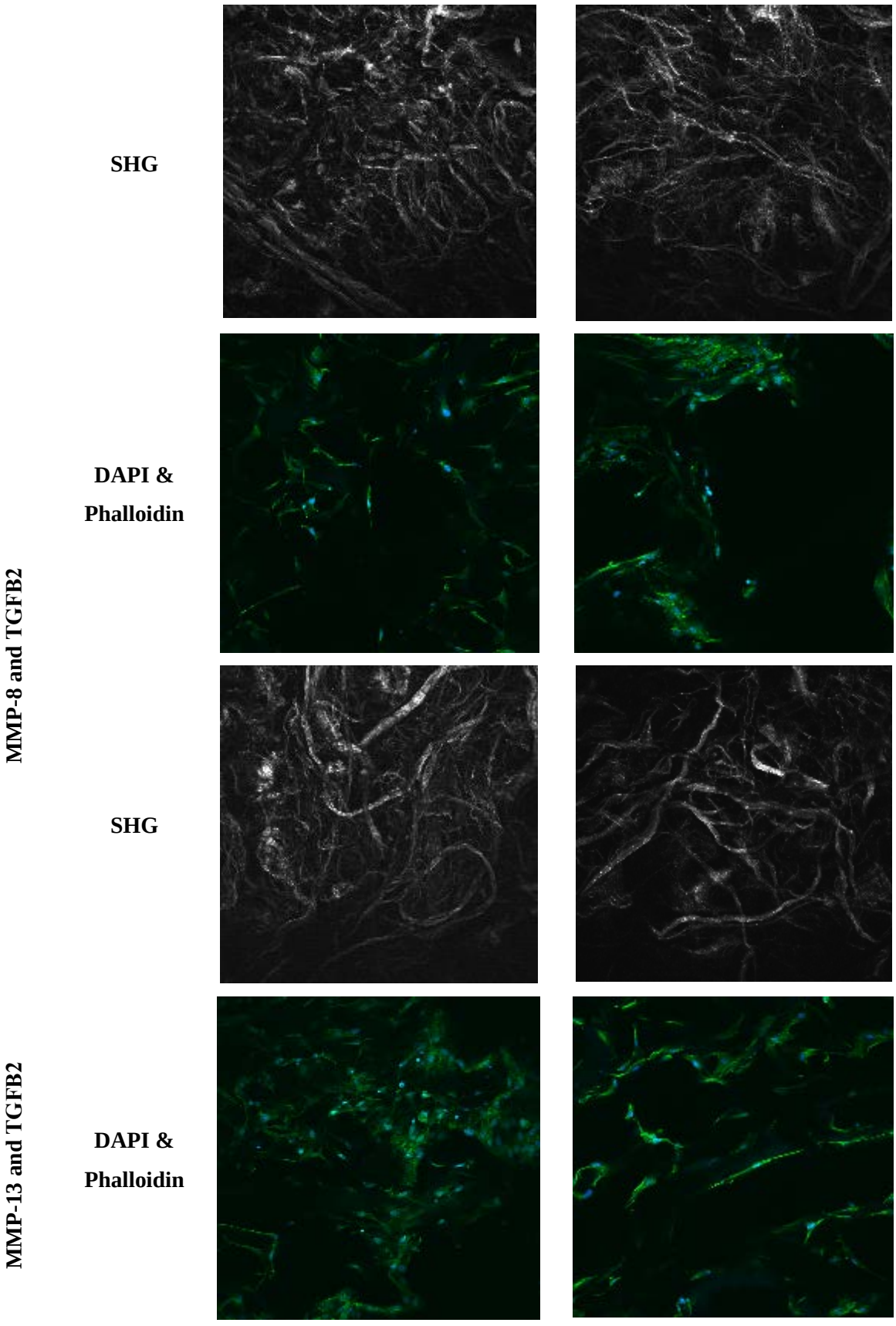
SHG
DAPI &
Phalloidin
MMP-8 and TGFB2
SHG
DAPI &
Phalloidin
MMP-13 and TGFB2

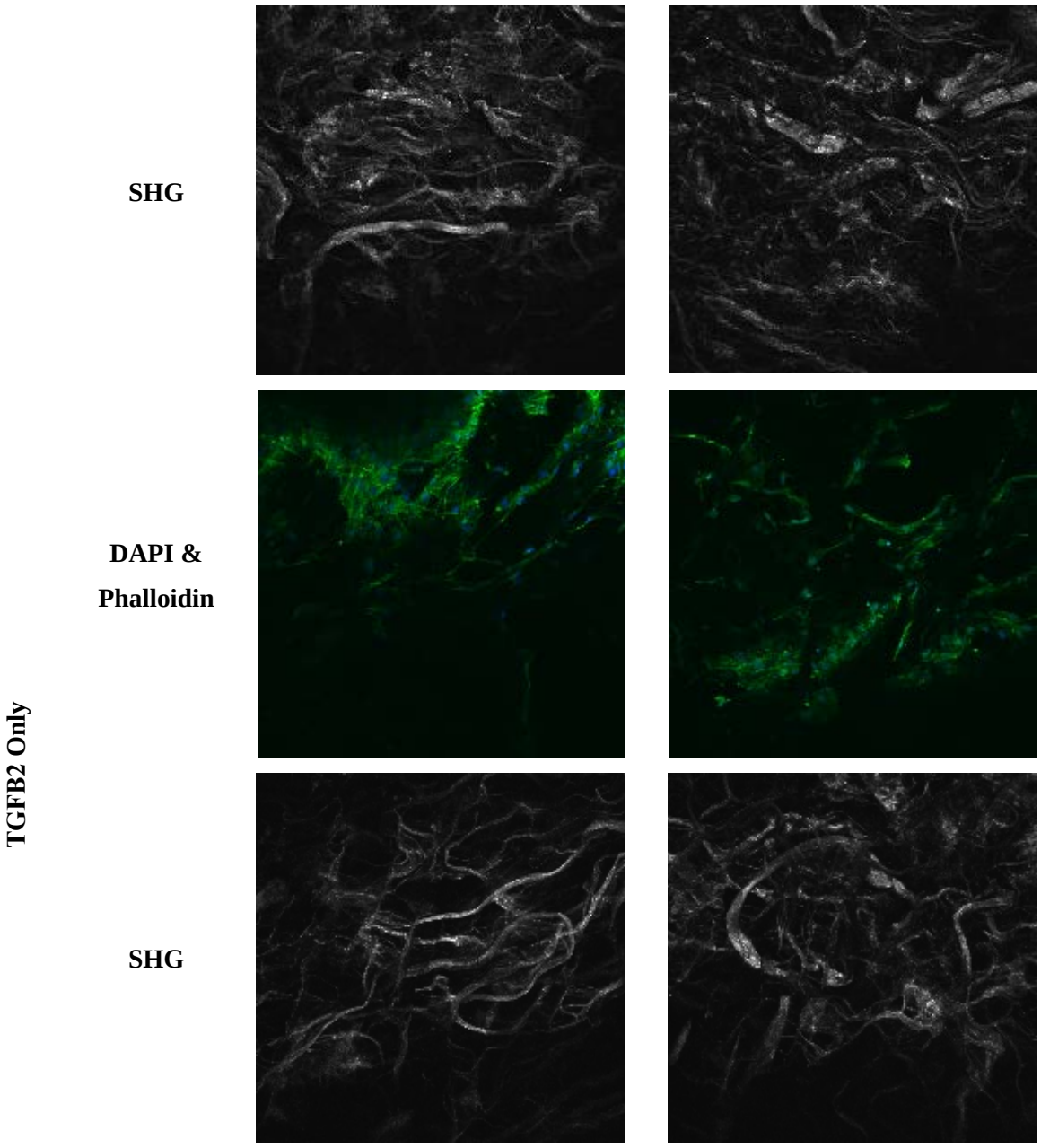

Figure 4.3: Collagen type I scaffolds treated with MMPs and TGFβ2. Scaffolds were imaged with SHG imaging (4x objective, black and white) and for cell nuclei and actin cytoskeleton (20x objective, green and blue).

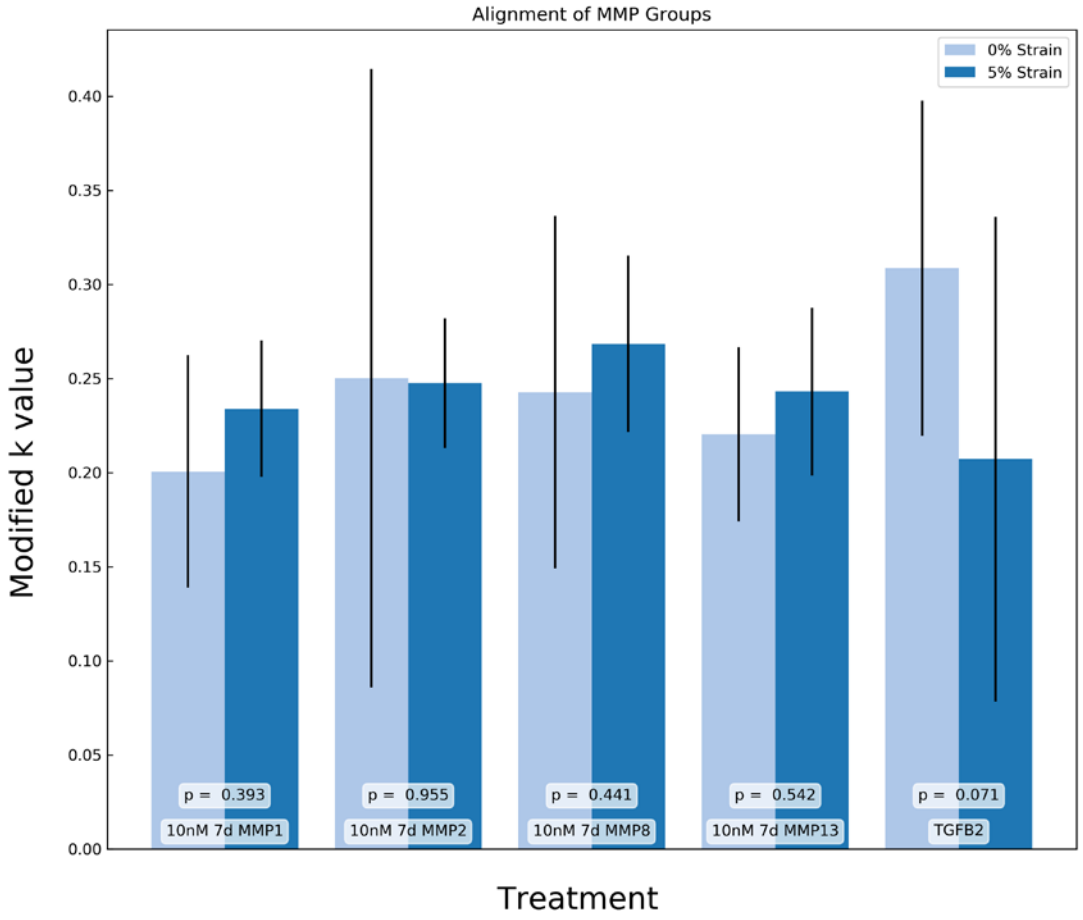

Figure 4.4: Fiberfit data showing the median fiber alignment (modified k value) for each MMP group and the TGFβ2 only groups. The p-values are reported on the bar graph for the groups.

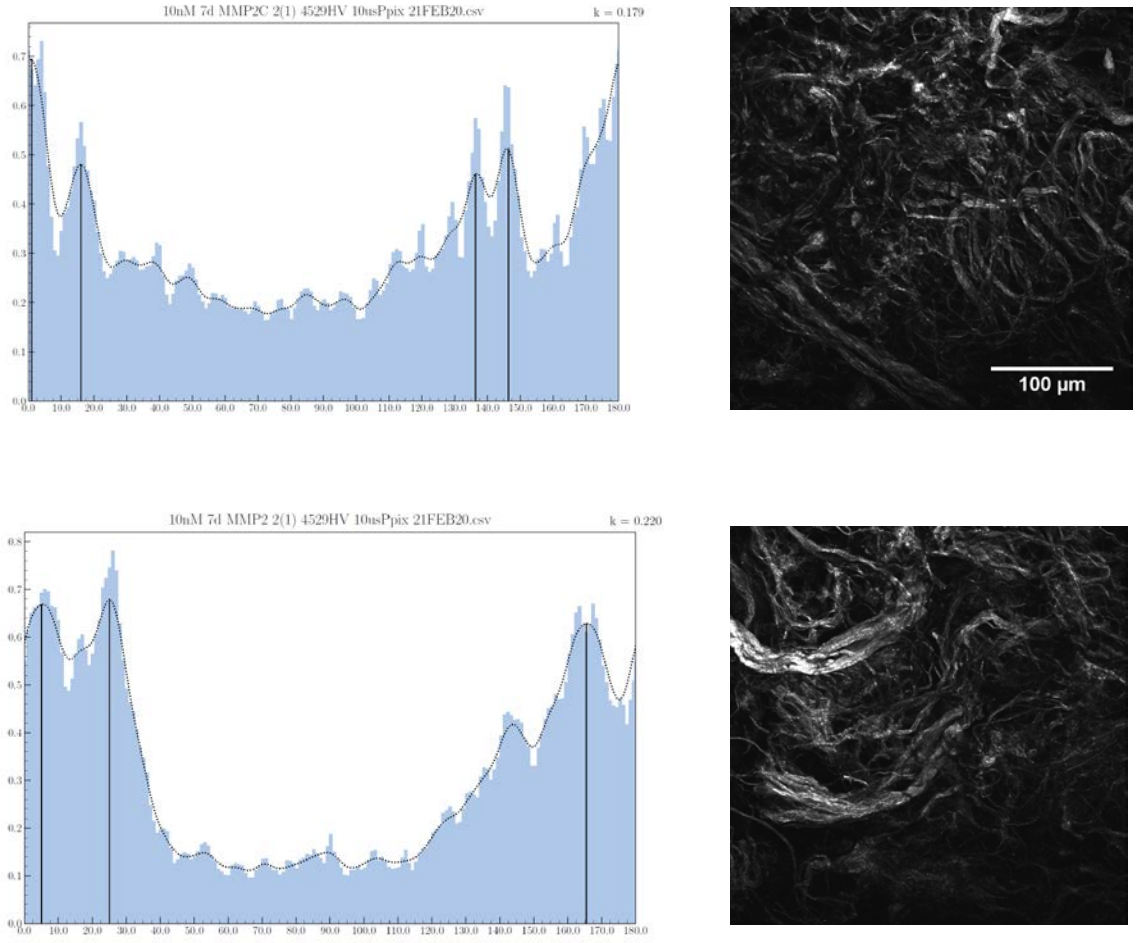

Figure 4.5: Histograms (left) generated from SHG images (right, 4x objective) by a modified version of Fiberfit. The y-axis shows normalized intensity. The x-axis shows degree of orientation. The modified alignment (k) is given for each histogram. The degree of alignment shown in each histogram can be seen in the SHG images. Top: MMP-2 with TGFβ2 + 0% strain. Bottom: MMP-2 with TGFβ2 + 5%.

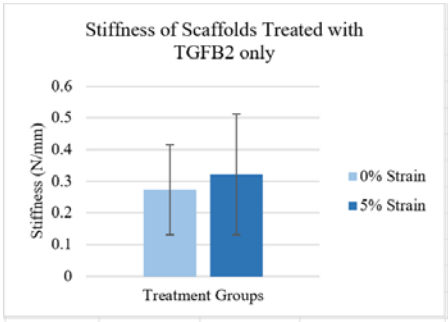
Stiffness of Scaffolds Treated with TGFB2 only
Stiffness (N/mm)
0.6
0.5
0.4
0.3
0.2
0.1
0
Treatment Groups
0% Strain
5% Strain

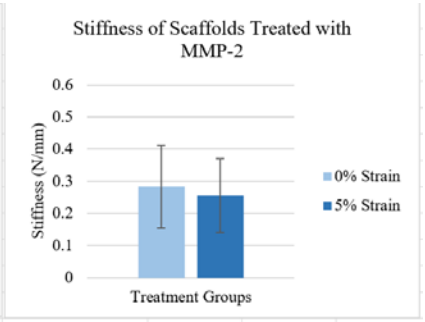
Stiffness of Scaffolds Treated with MMP-2
Stiffness (N/mm)
0.6
0.5
0.4
0.3
0.2
0.1
0
Treatment Groups
0% Strain
5% Strain

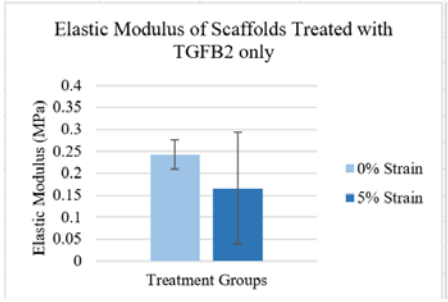
Elastic Modulus of Scaffolds Treated with TGFB2 only
Elastic Modulus (MPa)
0.4
0.35
0.3
0.25
0.2
0.15
0.1
0.05
0
Treatment Groups
0% Strain
5% Strain

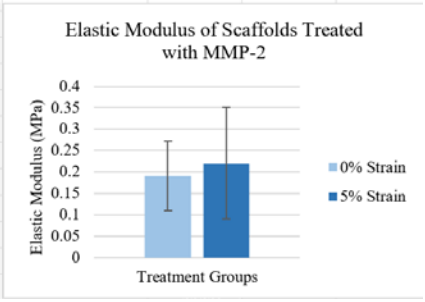
Elastic Modulus of Scaffolds Treated with MMP-2
Elastic Modulus (MPa)
0.4
0.35
0.3
0.25
0.2
0.15
0.1
0.05
0
Treatment Groups
0% Strain
5% Strain

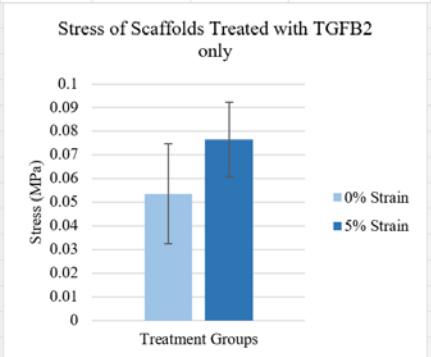
Stress of Scaffolds Treated with TGFB2 only
Stress (MPa)
0.1
0.09
0.08
0.07
0.06
0.05
0.04
0.03
0.02
0.01
0
Treatment Groups
0% Strain
5% Strain

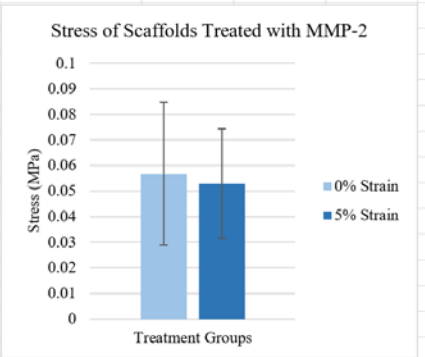
Stress of Scaffolds Treated with MMP-2
Stress (MPa)
0.1
0.09
0.08
0.07
0.06
0.05
0.04
0.03
0.02
0.01
0
Treatment Groups
0% Strain
5% Strain

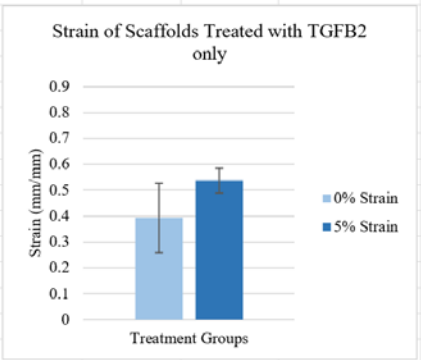
Strain of Scaffolds Treated with TGFB2 only
Strain (mm/mm)
0.9
0.8
0.7
0.6
0.5
0.4
0.3
0.2
0.1
0
Treatment Groups
0% Strain
5% Strain

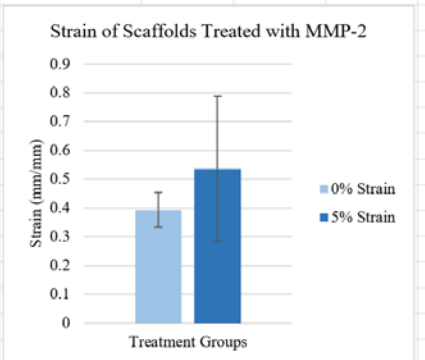
Strain of Scaffolds Treated with MMP-2
Strain (mm/mm)
0.9
0.8
0.7
0.6
0.5
0.4
0.3
0.2
0.1
0
Treatment Groups
0% Strain
5% Strain

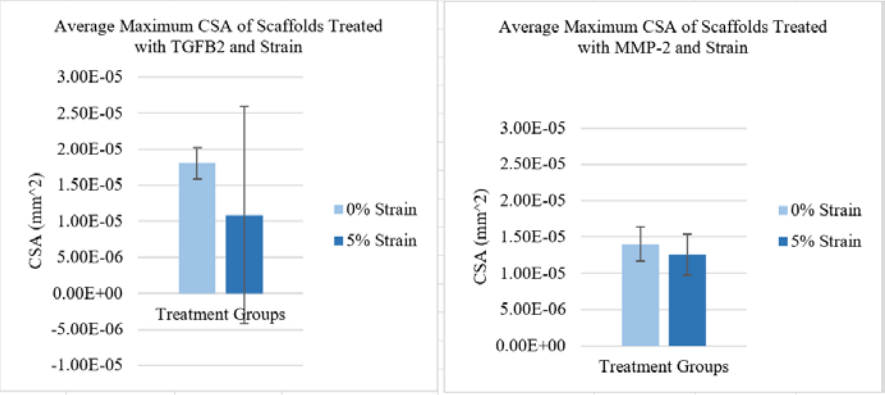

Figure 4.6: Results from mechanical testing scaffolds treated with TGFβ2 only and MMP-2 + TGFβ2 and had either 0% strain or 5% strain applied for 7 days. TGFβ2 only groups are shown on the left. MMP-2 + TGFβ2 groups are shown on the right.

Discussion

Mechanical tensile strain and active MMP treatments did not negatively impact tenogenically differentiating MSC growth in the collagen scaffolds. Interestingly, the MSCs in the MMP-2 + 5% strain groups were more fibroblastic than the controls. Also, we saw localized alignment occurring, discussed below. With the SHG images, we expected to see the collagen fibers more aligned in the groups that were strained at 5% and treated with active MMPs, since collagen in loaded tendons aligns itself in the direction of the strain and may be strain protected (7, 25, 52). The Fiberfit data was analyzed to determine if there were any differences that were not qualitatively visible. Each group treated with MMPs and 5% strain had higher alignment values (modified k values) than the control (0% strain) group, but no statistically significant differences were detected between the control and treatment groups. However, when looking at the histogram in Figure 4.5, the angle of alignment matches the angles of the collagen fibers in the SHG image, and localized alignments appear to be occurring approximately 145° from each other. However, quantification of the bulk histogram data is needed to confirm if these intervals are significant. This could fit with the finding that MMPs degrade unloaded collagen, and, in combination with the strain, preserve the aligned and strained collagen (7). It is also possible that the new collagen is deposited along the axis of strain (25). A limitation to this study is the highly disorganized and uncontrolled starting collagen network in the scaffolds. This highlights a main challenge for developing an engineered tendon replacement and highlights a challenge when making comparisons across treatment groups. Ideally, scaffolds could have been initially imaged with SHG, cultured with MSCs and treated with MMPs, and then re-imaged in the same exact location. This may be worth exploring in future studies but is challenging due to the need to maintain sterility and to image in the same location. The mechanical testing of the MMP-2 scaffolds (Figure 4.6) demonstrated a slightly increased stiffness and lower elastic modulus in the

control groups, but showed no statistically significant differences. Overall, the lack of changes in the mechanical properties suggests that mechanical properties were not impacted by the MMPs. It is also possible that the MMPs could have removed the unaligned collagen fibers, demonstrating that active MMP treatments have potential for improving localized collagen fiber alignment without being destructive or changing the mechanical function (7, 52).

From these findings, future directions include conducting tensile testing on scaffolds that have been treated with MMP-1, 8, and 13 + 5% strain, as well as repeating the test with the MMP-2 groups and an increased range of strain values, MMP concentrations, and timepoints. Furthermore, quantifying the angle intervals of localized alignment will be useful for determining any patterns that may be occurring.

Chapter 5: Conclusion and Future Directions

The main goal of this project was to understand the effects of exogenously applied MMPs on engineered tendon tissue formation *in vitro*. We explored MMP treatments of MSC-seeded collagen scaffolds, which have shown promise for tendon tissue engineering (33). Overall, these experiments provided useful preliminary data on how pro-form MMPs, active MMPs (with TGFβ2 induced tenogenesis of MSCs), and active MMPs combined with mechanical loading impact tissue formation in collagen scaffolds. We hypothesized that MMPs would promote the formation of an aligned collagen network for the purpose of developing a tissue engineered tendon.

Chapter Summaries

Chapter 2 describes experiments with collagen type I scaffolds seeded with MSCs and treated with four pro-form MMPs: MMP-1, MMP-2, MMP-8, and MMP-13. We hypothesized that adding the collagen degrading pro-form MMPs to the collagen type I scaffolds would result in collagen fiber degradation as well as a change in the collagen alignment. There were no statistically significant differences in the alignment (modified k values) between treatment and control groups. The fiber alignment of these scaffolds did not have much of a trend, but we may not expect a trend since the MMPs activity was not controlled. It is possible that systemic degradation that would not alter alignment occurred. This could be because MMPs were not activated and activation could be necessary to see the collagen degradation (27, 30). Therefore, Chapter 3 explored the use of activated MMPs, and Chapter 4 explored using the theory of strain protection to better control MMP-mediated collagen degradation.

Chapter 3 describes experiments with collagen type I scaffolds seeded with MSCs and active MMP-1, MMP-2, MMP-8, and MMP-13. Initially we treated MSCs in plates to ensure there was no cytotoxicity or change to cell viability and morphology. MMPs and TGFβ2 were added to the MSC seeded scaffolds and treated for 3 or 7 days with concentrations of either 1 nM or 10 nM. We found no visible changes to the collagen scaffolds and the cells appeared to proliferate as expected. There was no obvious trend in the alignment (modified k value) between treatment and control groups, and there were no statistically significant differences. There was no clear pattern of which groups had a higher alignment and which groups did not. It is possible that we did not see any clear results, again, due to tight MMP regulation by the tenogenically differentiating MSCs. However, it is more likely that the addition of MMPs into disorganized collagen makes it difficult to visualize and get meaningful quantitative alignment data. MMPs may also need some type of mechanical stimulation to better direct collagen degradation, which was explored in Chapter 4.

Chapter 4 describes how active MMP-1, MMP-2, MMP-8, MMP-13 in combination with tensile strain impacted collagen type I scaffolds seeded with tenogenically differentiating MSCs. The scaffolds were placed in seeding wells and strained in tension at either 0% (control) or 5%. It was predicted that the application of 5% strain to scaffolds treated with MMPs would result in a more aligned collagen network with the stretch direction (25), and have higher modified k values. No groups were statistically significant from one another. The histogram for active MMP-2 + 5% and 0% strain showed the angles where collagen alignment was highest, and fibers appeared more aligned along localized angles with strain. Active MMP-2 + 5% strain and TGFβ2 was chosen for conducting tensile testing, as MMP-2 has been shown to be at high levels in developing embryonic tendon (23). Since mechanical cues and loading are critical to tendon development, we hypothesized that the mechanical properties of collagen type I scaffolds treated with MMP-2 and 5% strain would be altered compared to scaffolds treated with MMP-2 + 0% strain (5). No statistically significant differences between the different strain groups in the mechanical properties were found. This suggests that localized changes in the collagen alignment with active MMP-2 treatment did not impact the overall mechanical properties, demonstrating that the MMPs are not being overly destructive.

Key Conclusions

The main take-aways from this project are stated in the table below.

Table 5.1. Description of the three key conclusions from this project.

Conclusion 1	MMPs have been underexplored in tendon tissue engineering approaches despite their presence in embryonic tendon formation (23).
Conclusion 2	Exogenous MMP treatments of MSC-seeded collagen scaffolds are a possible treatment strategy to enhance tissue formation based on: 1. Maintained cell viability 2. Qualitative improvements in localized fiber alignment 3. Maintained mechanical properties
Conclusion 3	Combining strain and active MMPs with MSC-seeded collagen scaffolds may take advantage of the *Strain Protection Theory* for developing a more aligned collagen fiber network in collagen scaffolds

Future Directions

It is possible that the MSCs are inhibiting the MMPs, possibly through TIMPs (7, 19). Treating these same scaffolds with MMPs 1, 2, 8, and 13 without MSCs may provide additional useful data. Prevention of the MMP inhibitory properties (e.g., TIMPs) of MSCs could provide a useful mechanism for encouraging MMP activity and accelerated scaffold remodeling. To better understanding what role MMPs are playing in engineering tendon tissue formation, blocking MMPs

using the MMP inhibitor GM6001 is also worth exploring (19, 51). For tissue formation, MMPs may require the proper balance of inhibition and activation for their properties to be apparent (51). It might also be worth using zymography to measure the MMP activity, since the MMPs may have been inactivated by the MSCs (32).

Using another collagen scaffold could be useful. The collagen scaffolds used in these experiments are commonly used in tendon tissue engineering. However, it is possible the crosslinking of the collagen in the scaffolds reduced the ability for the MMPs to rapidly digest the collagen. Experimentation with other collagen scaffolds is needed.

Localized alignment was occurring at specific angle intervals. Quantifying the angle of alignment would be useful to see if there are any trends in how the collagen fibers are aligning. It is possible that these angles could be significant to collagen remodeling and tendon development. For example, alignment occurring at angles 90° from each other may be demonstrating the crimp pattern that we see in the collagen fibers of tendon. Fiberfit is a useful tool for analyzing images that produce a single peak, but a better method is needed for analyzing images that produce multi-modal histograms, such as images produced from these experiments.

A tissue engineered tendon is still needed to help the many people with tendon injuries. While additional work is needed to achieve a functional tendon replacement, the preliminary data described here is essential for moving forward as it provides new information on how MMPs may be used for guiding tendon formation. Continued research will be important to better understand what factors are needed for developing the ideal tendon replacement.

Literature Cited

1. Costa-Almeida, R., Clejo, I., Gomes, M.E. (2019). Mesenchymal stem cells empowering tendon regenerative therapies. *International Journal of Molecular Sciences, 20(12).*
2. Rumian, A., Wallace, A., Birch, L. (2006). Tendons and ligaments are anatomically distinct but overlap in molecular and morphological features—a comparative study in an ovine model. *Wiley InterScience,* 20218, 458-464.
3. Theodossiou, S., Schiele, N. 2019. Models of tendon development and injury. *BMC Biomedical Engineering*. 32.
4. Provenzano, P. P. and R. Vanderby, Jr. (2006). "Collagen fibril morphology and organization: implications for force transmission in ligament and tendon." *Matrix Biol,* 25(2): 71-84.
5. Brown, J. P., Finley, V. G., & Kuo, C. K. (2014). Embryonic mechanical and soluble cues regulate tendon progenitor cell gene expression as a function of developmental stage and anatomical origin. *Journal of Biomechanics*, *47*(1), 214–222.
6. Theodossiou, S. K., Tokle, J., & Schiele, N. R. (2019). TGFβ2-induced tenogenesis impacts cadherin and connexin cell-cell junction proteins in mesenchymal stem cells. *Biochemical and Biophysical Research Communications*, *508*(3), 889–893.
7. Flynn, B. P., Bhole, A. P., Saeidi, N., Liles, M., DiMarzio, C. A., & Ruberti, J. W. (2010). Mechanical Strain Stabilizes Reconstituted Collagen Fibrils against Enzymatic Degradation by Mammalian Collagenase Matrix Metalloproteinase 8 (MMP-8). *PLoS ONE*, *5*(8), e12337.
8. Davis, M. E., Gumucio, J. P., Sugg, K. B., Bedi, A., & Mendias, C. L. (2013). MMP inhibition as a potential method to augment the healing of skeletal muscle and tendon extracellular matrix. *J Appl Physiol*, *115*, 884–891.
9. Dong, C., Lv, Y., (2016). Application of collagen scaffold in tissue engineering: recent advances and new perspectives. *Polymers, 8(2).*
10. Kuo, C. K., Petersen, B. C., & Tuan, R. S. (2008). Spatiotemporal protein distribution of TGF-βs, their receptors, and extracellular matrix molecules during embryonic tendon development. *Developmental Dynamics*, *237*(5), 1477–1489.
11. Schiele, N. (2019). Tissue engineering and regenerative medicine notes.
12. Makris, E., Gomoll, A., Malizos, K., Hu, J., Athanasiou, K. (2015*).* Repair and tissue engineering techniques for articular cartilage. *Nat Rev Rheumatol, 11(1),* 21–34.
13. Rosenbaum, A., Grande, D., Dines, J. (2008). The use of mesenchymal stem cells in tissue engineering. *Organogenesis,* 4(1), 23-27.

14. Reznikoff, C., Brankow, D., & Heidelberger, C. (1973*).* Establishment and Characterization of a Cloned Line of C3H Mouse Embryo Cells Sensitive to Postconfluence Inhibition of Division. *Cancer Research,* 33, 3231-3238.
15. Li, S., Wu, J. (2020). TGF-β/SMAD signaling regulation of mesenchymal stem cells in adipocyte commitment. *Stem Cell Research & Therapy*.
16. Havis, E., Bonnin, M.-A., Esteves de Lima, J., Charvet, B., Milet, C., & Duprez, D. (2016). TGFβ and FGF promote tendon progenitor fate and act downstream of muscle contraction to regulate tendon differentiation during chick limb development. *Development*, *143*(20), 3839–3851.
17. Hadler-Olsen, E., Fadnes, B., Sylte, I., Uhlin-Hansen, L., & Winberg, J.-O. (2011). Regulation of matrix metalloproteinase activity in health and disease. *FEBS Journal*, *278*(1), 28–45.
18. Nagase, H., Visse, R., & Murphy, G. (2006). Structure and function of matrix metalloproteinases and TIMPs. *Cardiovascular Research*, *69*(3), 562–573.
19. Kasper, G., Glaeser, J. D., Geissler, S., Ode, A., Tuischer, J., Matziolis, G., Duda, G. N. (2007). Matrix Metalloprotease Activity Is an Essential Link Between Mechanical Stimulus and Mesenchymal Stem Cell Behavior. *Stem Cells*, *25*(8), 1985–1994.
20. Lindstad, R. I., Sylte, I., Mikalsen, S.-O., Seglen, P. O., Berg, E., & Winberg, J.-O. (2005). Pancreatic Trypsin Activates Human Promatrix Metalloproteinase-2. *Journal of Molecular Biology*, *350*(4), 682–698.
21. Zhang, J., & Wang, J. H. C. (2013). The Effects of Mechanical Loading on Tendons - An In Vivo and In Vitro Model Study. *PLoS ONE*, *8*(8), e71740.
22. Khayyeri, H., Blomgran, P., Hammerman, M., Turunen, M., Lowgren, A., Guizar-Sicairos, M., Aspenberg, P., & Isaksson, H. (2017). Achilles tendon compositional and structural properties are altered after unloading by botox. *Scientific Reports, 7(13067).*
23. Jung, J., Wang, P., Zhang, G., Ezura, Y., Fini, M. Birk, D. (2009). Collagen fibril growth during chicken tendon development: matrix metalloproteinase-2 and its activation. *Cell Tissue Res., 336(1)*; 79-89.
24. Buono, A., Oliva, F., Osti, L., Maffulli, N. (2013). Metalloproteases and tendinopathy. *Muscles Ligaments Tendons J., 3(1);* 51-57.
25. Ghazanfari, S., Driessen-Mol, A., Bouten, C.V.C., & Baaijens, F.P.T. (2015). Modulation of collagen fiber orientation by strain-controlled enzymatic degradation. *Acta Biomaterialia.*
26. Brown, J. P., Galassi, T. V., Stoppato, M., Schiele, N. R., & Kuo, C. K. (2015). Comparative analysis of mesenchymal stem cell and embryonic tendon progenitor cell response to embryonic tendon biochemical and mechanical factors. *Stem Cell Research & Therapy*, *6*(1), 89.

27. Loffek, S., Schilling, O., & Franzke, C-W. (2011). Biological role of matrix metalloproteinases: a critical balance. *Eur Respir J.,* 38. 191-208.
28. Morill, E., Tulepbergenov, A., Stender, C., Lamichhane, R., Brown, R., & Lujan, T. (2016). A validated software application to measure fiber organization in soft tissue. *Biomech Model Mechanobiol.,* 15(6). 1467-1478.
29. Lozito, T. P., Jackson, W. M., Nesti, L. J., & Tuan, R. S. (2014). Human mesenchymal stem cells generate a distinct pericellular zone of MMP activities via binding of MMPs and secretion of high levels of TIMPs. *Matrix Biology*, *34*, 132–143.
30. Jabłońska-Trypuć, A., Matejczyk, M., & Stanisław Rosochacki. (2016). Matrix metalloproteinases (MMPs), the main extracellular matrix (ECM) enzymes in collagen degradation, as a target for anticancer drugs, *Journal of Enzyme Inhibition and Medicinal Chemistry,* 31:sup1, 177-183.
31. Chondrex. (2018). Collagenase assay kit. *Chondrex*.
32. Hu, X., & Beeton, C. (2010). Detection of Functional Matrix Metalloproteinases by Zymography. *Journal of Visualized Experiments*, (45).
33. Butler, D., Gooch, C., Kinneberg, KR., Boivin, GP., Nirmalanandhan, VS., Shearn, JT., Dyment, NA., Juncosa-Melvin, N. The use of mesenchymal stem cells in collagen-based scaffolds for tissue-engineered repair of tendons. *Nat Protoc*.. 5(5); 849-863.
34. Risinger, M., Schiele, N. 2017. Investigating the effects of static tensile strain and enzymatic degradation on collagen fiber alignment. *Idaho INBRE Conference*. Poster Presentation.
35. Russo V, Mauro A, Martelli A, Di Giacinto O, Di Marcantonio L, Nardinocchi D, et al. 2015. Cellular and molecular maturation in fetal and adult ovine calcaneal tendons. *J Anat.*, 226(2):126–42.
36. Richardson SH, Starborg T, Lu Y, Humphries SM, Meadows RS, Kadler KE. 2007. Tendon development requires regulation of cell condensation and cell shape via cadherin-11-mediated cell-cell junctions. *Mol Cell Biol*., 27(17):6218–28.
37. Apte SS, Fukai N, Beier DR, Olsen BR. 1997. The matrix metalloproteinase-14 (MMP-14) gene is structurally distinct from other MMP genes and is co-expressed with the TIMP-2 gene during mouse embryogenesis. *J Biol Chem*., 272(41):25511–7.
38. Kinoh H, Sato H, Tsunezuka Y, Takino T, Kawashima A, Okada Y, et al. 1996. MT-MMP, the cell surface activator of proMMP-2 (pro-gelatinase a), is expressed with its substrate in mouse tissue during embryogenesis. *J Cell Sci*., 109(Pt 5):953–9.
39. Edom-Vovard F, Schuler B, Bonnin MA, Teillet MA, Duprez D. 2002. Fgf4 positively regulates scleraxis and tenascin expression in chick limb tendons. *Dev Biol*., 247(2):351–66.

40. Kieny M, Chevallier A. 1979. Autonomy of tendon development in the embryonic chick wing. *J Embryol Exp Morphol*., 49:153–65.
41. Pan XS, Li J, Brown EB, Kuo CK. 2018. Embryo movements regulate tendon mechanical property development. *Phil. Trans*., R. Soc. B. 373:20170325.
42. Glass ZA, Schiele NR, Kuo CK. 2014. Informing tendon tissue engineering with embryonic development. *J Biomech*., 47:1964–8.
43. Dyment NA, Galloway JL. 2015. Regenerative biology of tendon: mechanisms for renewal and repair. *Curr Mol Biol Rep*., 1(3):124–31.
44. Pryce BA, Watson SS, Murchison ND, Staverosky JA, Dunker N, Schweitzer R. 2009. Recruitment and maintenance of tendon progenitors by TGFbeta signaling are essential for tendon formation. Development.136(8):1351–61.
45. Kuo CK, Tuan RS. 2008. Mechanoactive tenogenic differentiation of human mesenchymal stem cells. *Tissue Eng Part A*., 14(10):1615–27.
46. Subramony SD, Dargis BR, Castillo M, Azeloglu EU, Tracey MS, Su A, et al. 2013. The guidance of stem cell differentiation by substrate alignment and mechanical stimulation. *Biomaterials*, 34(8):1942–53.
47. Chokalingam K, Juncosa-Melvin N, Hunter SA, Gooch C, Frede C, Florert J, et al. 2009. Tensile stimulation of murine stem cell-collagen sponge constructs increases collagen type I gene expression and linear stiffness. *Tissue Eng Part A*., 15(9):2561–70.
48. Juncosa-Melvin N, Matlin KS, Holdcraft RW, Nirmalanandhan VS, Butler DL. 2007. Mechanical stimulation increases collagen type I and collagen type III gene expression of stem cell-collagen sponge constructs for patellar tendon repair. *Tissue Eng.*, 13(6):1219–26.
49. Heinemeier KM, Skovgaard D, Bayer ML, Qvortrup K, Kjaer A, Kjaer M, et al. 2012. Uphill running improves rat Achilles tendon tissue mechanical properties and alters gene expression without inducing pathological changes. *J Appl Physiol*., 113:827–36.
50. Goodman SA, May SA, Heinegard D, Smith RK. 2004. Tenocyte response to cyclical strain and transforming growth factor beta is dependent upon age and site of origin. *Biorheology*,41(5):613–28.
51. Arnoczky SP, Lavagnino M, Egerbacher M, Caballero O, Gardner K. 2007. Matrix metalloproteinase inhibitors prevent a decrease in the mechanical properties of stress-deprived tendons - An in vitro experimental study. *Am J Sports Med.*, 35(5):763–9.
52. Bhole AP, Flynn BP, Liles M, Saeidi N, Dimarzio CA, Ruberti JW. 2009. Mechanical strain enhances survivability of collagen micronetworks in the presence of collagenase: implications for

load-bearing matrix growth and stability. *Philos Transact A Math Phys Eng Sci*., 367(1902):3339–62.

53. Wyatt, K. E., et al. (2009). "Deformation-dependent enzyme mechanokinetic cleavage of type I collagen." *J Biomech Eng*., 131(5): 051004.
54. Nirmalanandhan, V. S., et al. (2008). "Effect of scaffold material, construct length and mechanical stimulation on the in vitro stiffness of the engineered tendon construct." *J Biomech.*, 41(4): 822-828.
55. Marturano, J. E., et al. (2016). "Embryonically inspired scaffolds regulate tenogenically differentiating cells." *J Biomech*., 49(14): 3281-3288.

Appendix A. Supplemental Tables and Figures

Table A.1: Comparisons of the p values for the modified k values for active MMP 1, 2, 8, and 13. Each group was compared to every time point and concentration, and p-values are show. Statistical significance is determined by $p < 0.05$. No comparisons were statistically significant.

Groups: Active MMP-1	P-values
Treatment :1nM 7d vs. Treatment :1nM 3d	>0.9999
Treatment :10nM 3d vs. Treatment :1nM 3d	0.6934
Treatment :10nM 7d vs. Treatment :1nM 3d	0.6464
Control :1nM 3d vs. Treatment :1nM 3d	0.9801
Control :1nM 7d vs. Treatment :1nM 3d	0.9998
Control :10nM 3d vs. Treatment :1nM 3d	>0.9999
Control :10nM 7d vs. Treatment :1nM 3d	0.888
Treatment :10nM 3d vs. Treatment :1nM 7d	0.5278
Treatment :10nM 7d vs. Treatment :1nM 7d	0.4814
Control :1nM 3d vs. Treatment :1nM 7d	0.9219
Control :1nM 7d vs. Treatment :1nM 7d	0.995
Control :10nM 3d vs. Treatment :1nM 7d	0.9982
Control :10nM 7d vs. Treatment :1nM 7d	0.7572
Treatment :10nM 7d vs. Treatment :10nM 3d	>0.9999
Control :1nM 3d vs. Treatment :10nM 3d	0.9922
Control :1nM 7d vs. Treatment :10nM 3d	0.9037
Control :10nM 3d vs. Treatment :10nM 3d	0.8625
Control :10nM 7d vs. Treatment :10nM 3d	0.9999
Control :1nM 3d vs. Treatment :10nM 7d	0.9863
Control :1nM 7d vs. Treatment :10nM 7d	0.8736
Control :10nM 3d vs. Treatment :10nM 7d	0.8265
Control :10nM 7d vs. Treatment :10nM 7d	0.9996
Control :1nM 7d vs. Control :1nM 3d	0.9996
Control :10nM 3d vs. Control :1nM 3d	0.9986
Control :10nM 7d vs. Control :1nM 3d	>0.9999
Control :10nM 3d vs. Control :1nM 7d	>0.9999
Control :10nM 7d vs. Control :1nM 7d	0.9861
Control :10nM 7d vs. Control :10nM 3d	0.9734

Groups: Active MMP-2	P-values
Treatment :1nM 3d vs. Treatment :1nM 7d	0.1921
Treatment :1nM 3d vs. Treatment :10nM 3d	0.9998
Treatment :1nM 3d vs. Treatment :10nM 7d	>0.9999
Treatment :1nM 3d vs. Control :1nM 3d	>0.9999
Treatment :1nM 3d vs. Control :1nM 7d	>0.9999
Treatment :1nM 3d vs. Control :10nM 3d	>0.9999
Treatment :1nM 3d vs. Control :10nM 7d	0.9284
Treatment :1nM 7d vs. Treatment :10nM 3d	0.0941
Treatment :1nM 7d vs. Treatment :10nM 7d	0.2604
Treatment :1nM 7d vs. Control :1nM 3d	0.1264
Treatment :1nM 7d vs. Control :1nM 7d	0.3111
Treatment :1nM 7d vs. Control :10nM 3d	0.2613
Treatment :1nM 7d vs. Control :10nM 7d	0.0229
Treatment :10nM 3d vs. Treatment :10nM 7d	0.9982
Treatment :10nM 3d vs. Control :1nM 3d	>0.9999
Treatment :10nM 3d vs. Control :1nM 7d	0.9944
Treatment :10nM 3d vs. Control :10nM 3d	0.9981
Treatment :10nM 3d vs. Control :10nM 7d	0.9933
Treatment :10nM 7d vs. Control :1nM 3d	0.9998
Treatment :10nM 7d vs. Control :1nM 7d	>0.9999
Treatment :10nM 7d vs. Control :10nM 3d	>0.9999
Treatment :10nM 7d vs. Control :10nM 7d	0.8587
Control :1nM 3d vs. Control :1nM 7d	0.9989
Control :1nM 3d vs. Control :10nM 3d	0.9998
Control :1nM 3d vs. Control :10nM 7d	0.9789
Control :1nM 7d vs. Control :10nM 3d	>0.9999
Control :1nM 7d vs. Control :10nM 7d	0.8026
Control :10nM 3d vs. Control :10nM 7d	0.8577

Groups: Active MMP-8	P-values
Treatment :1nM 3d vs. Treatment :1nM 7d	0.1227
Treatment :1nM 3d vs. Treatment :10nM 3d	0.8642
Treatment :1nM 3d vs. Treatment :10nM 7d	0.3753
Treatment :1nM 3d vs. Control :1nM 3d	>0.9999
Treatment :1nM 3d vs. Control :1nM 7d	0.9235
Treatment :1nM 3d vs. Control :10nM 3d	0.9855
Treatment :1nM 3d vs. Control :10nM 7d	>0.9999
Treatment :1nM 7d vs. Treatment :10nM 3d	0.7379
Treatment :1nM 7d vs. Treatment :10nM 7d	0.9951
Treatment :1nM 7d vs. Control :1nM 3d	0.1851
Treatment :1nM 7d vs. Control :1nM 7d	0.643
Treatment :1nM 7d vs. Control :10nM 3d	0.4527
Treatment :1nM 7d vs. Control :10nM 7d	0.1995
Treatment :10nM 3d vs. Treatment :10nM 7d	0.9824
Treatment :10nM 3d vs. Control :1nM 3d	0.945
Treatment :10nM 3d vs. Control :1nM 7d	>0.9999
Treatment :10nM 3d vs. Control :10nM 3d	0.9995
Treatment :10nM 3d vs. Control :10nM 7d	0.9556
Treatment :10nM 7d vs. Control :1nM 3d	0.5079
Treatment :10nM 7d vs. Control :1nM 7d	0.9568
Treatment :10nM 7d vs. Control :10nM 3d	0.8513
Treatment :10nM 7d vs. Control :10nM 7d	0.5349
Control :1nM 3d vs. Control :1nM 7d	0.976
Control :1nM 3d vs. Control :10nM 3d	0.998
Control :1nM 3d vs. Control :10nM 7d	>0.9999
Control :1nM 7d vs. Control :10nM 3d	>0.9999
Control :1nM 7d vs. Control :10nM 7d	0.9818
Control :10nM 3d vs. Control :10nM 7d	0.9988

Groups: Active MMP-13	P-values
Treatment :1nM 3d vs. Treatment :1nM 7d	0.1468
Treatment :1nM 3d vs. Treatment :10nM 3d	0.1616
Treatment :1nM 3d vs. Treatment :10nM 7d	0.1014
Treatment :1nM 3d vs. Control :1nM 3d	0.9761
Treatment :1nM 3d vs. Control :1nM 7d	0.0407
Treatment :1nM 3d vs. Control :10nM 3d	0.128
Treatment :1nM 3d vs. Control :10nM 7d	0.0605
Treatment :1nM 7d vs. Treatment :10nM 3d	>0.9999
Treatment :1nM 7d vs. Treatment :10nM 7d	>0.9999
Treatment :1nM 7d vs. Control :1nM 3d	0.56
Treatment :1nM 7d vs. Control :1nM 7d	0.9954
Treatment :1nM 7d vs. Control :10nM 3d	>0.9999
Treatment :1nM 7d vs. Control :10nM 7d	0.9995
Treatment :10nM 3d vs. Treatment :10nM 7d	>0.9999
Treatment :10nM 3d vs. Control :1nM 3d	0.594
Treatment :10nM 3d vs. Control :1nM 7d	0.9927
Treatment :10nM 3d vs. Control :10nM 3d	>0.9999
Treatment :10nM 3d vs. Control :10nM 7d	0.999
Treatment :10nM 7d vs. Control :1nM 3d	0.4381
Treatment :10nM 7d vs. Control :1nM 7d	0.9995
Treatment :10nM 7d vs. Control :10nM 3d	>0.9999
Treatment :10nM 7d vs. Control :10nM 7d	>0.9999
Control :1nM 3d vs. Control :1nM 7d	0.2159
Control :1nM 3d vs. Control :10nM 3d	0.5132
Control :1nM 3d vs. Control :10nM 7d	0.298
Control :1nM 7d vs. Control :10nM 3d	0.9978
Control :1nM 7d vs. Control :10nM 7d	>0.9999
Control :10nM 3d vs. Control :10nM 7d	0.9998

Group: 3d	1nM Control	1 nM
MMP-1	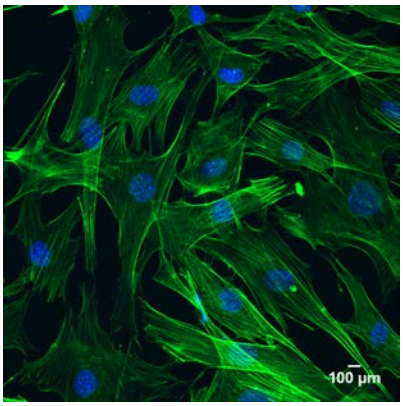	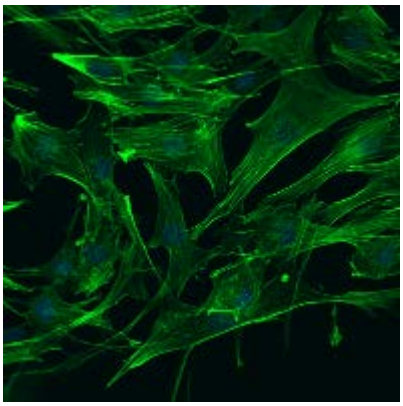
MMP-2	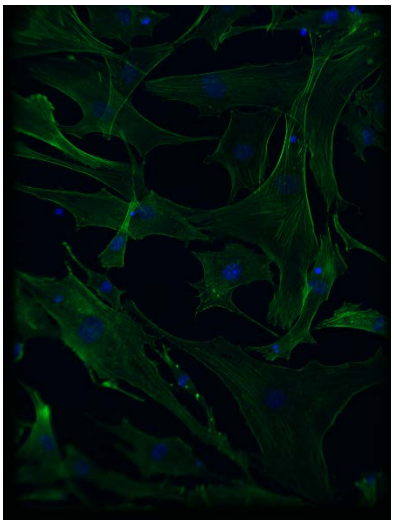	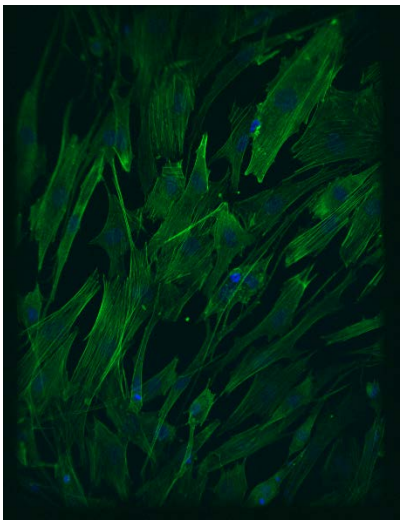
MMP-8	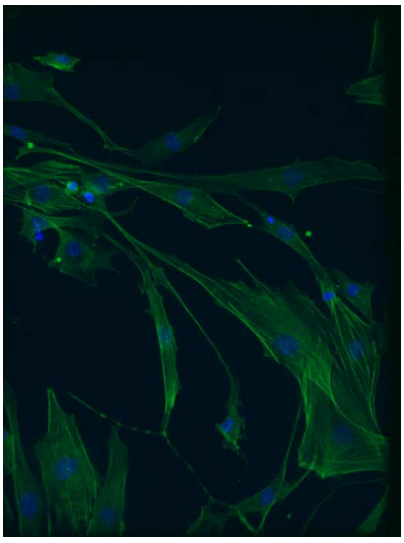	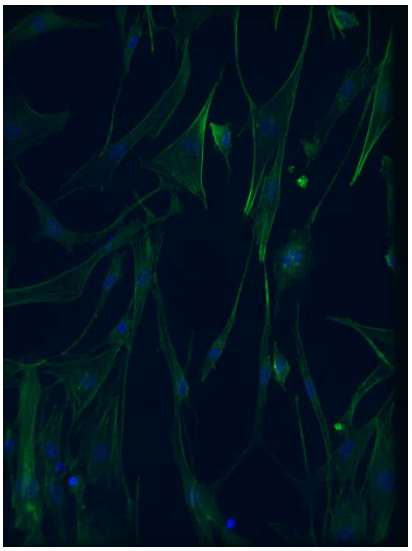

MMP-13

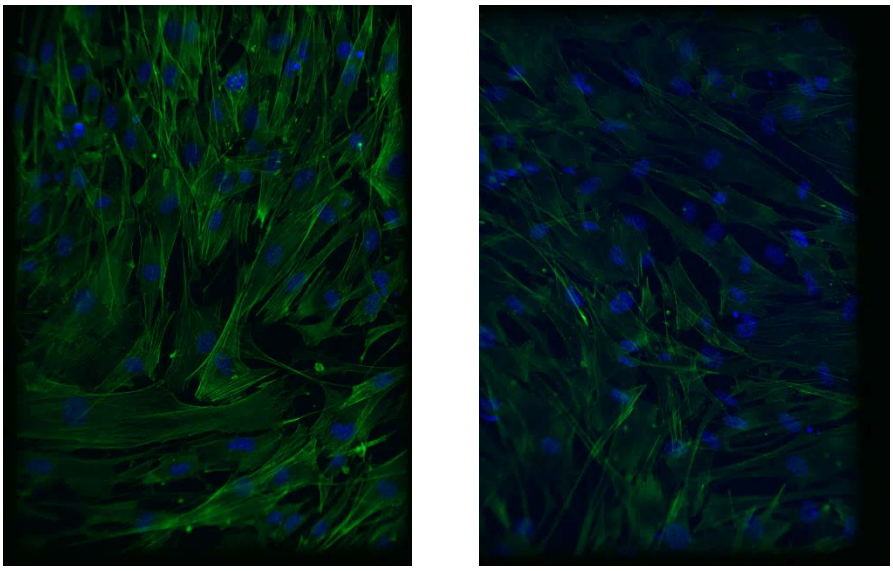

Figure A.1: Images (20x objective) of cover slips stained with DAPI and Phalloidin and treated with 1 nM of MMP-1, 2, 8, or 13 for 3 days.

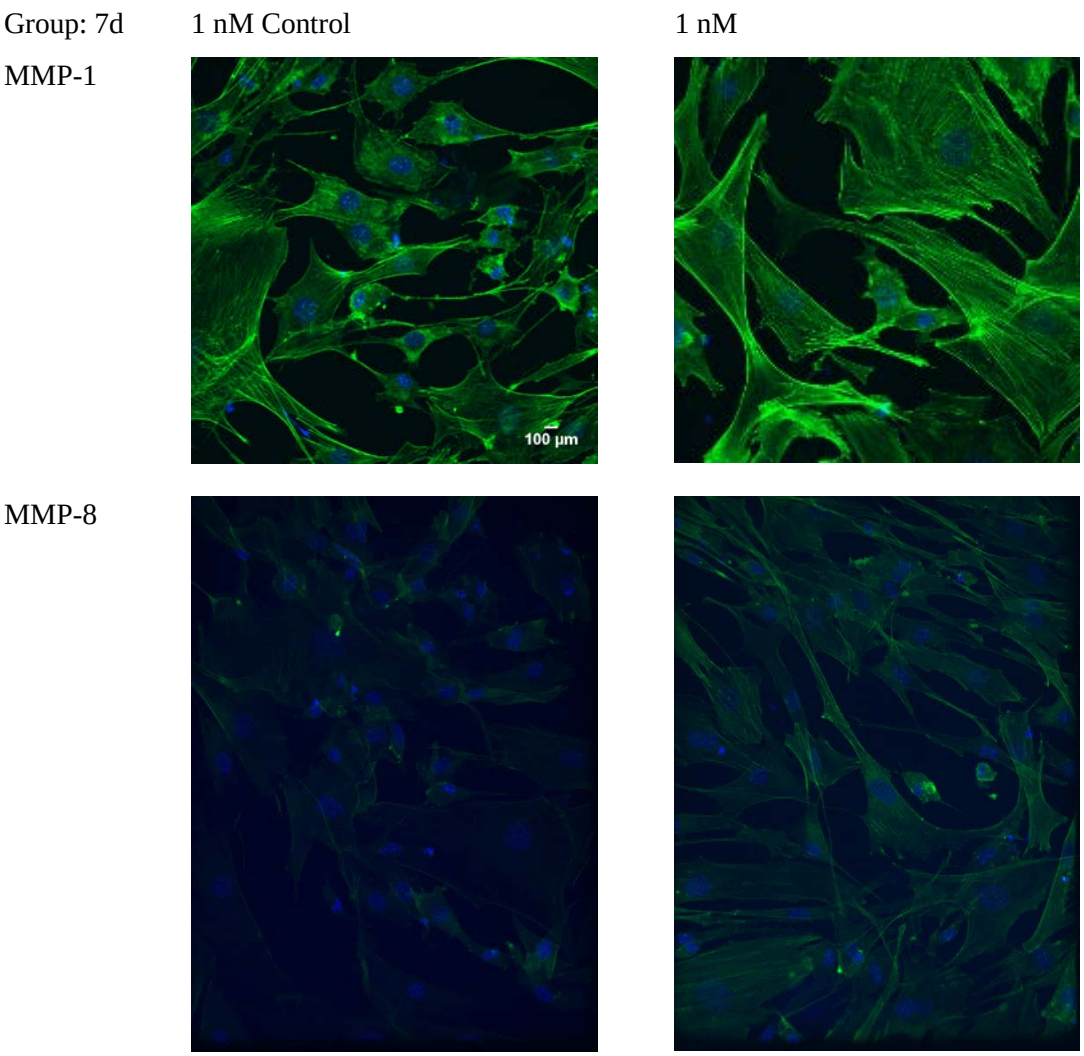

Figure A.2. Images (20x objective) of cover slips stained with DAPI and Phalloidin and treated with 1nM of MMP-1 and 8 for 7 days.

Group: 3d	10 nM Control	10 nM
MMP-1	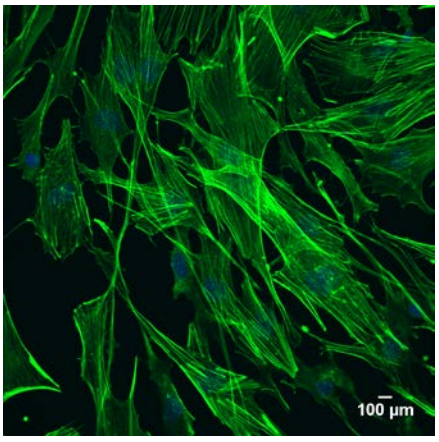	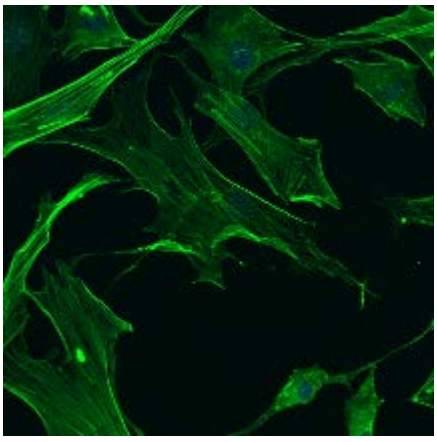
MMP-2	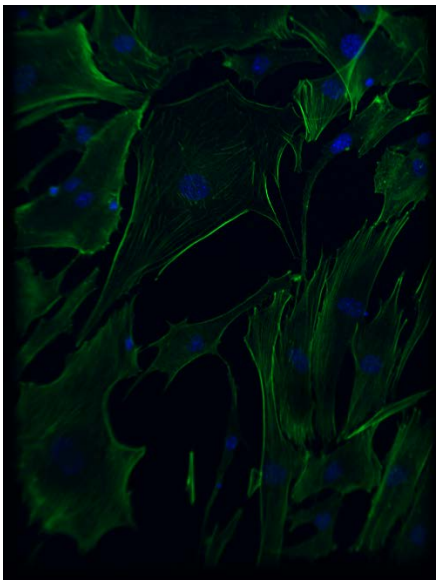	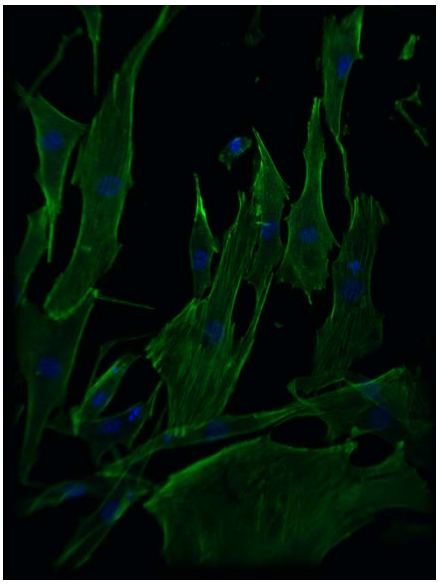
MMP-8	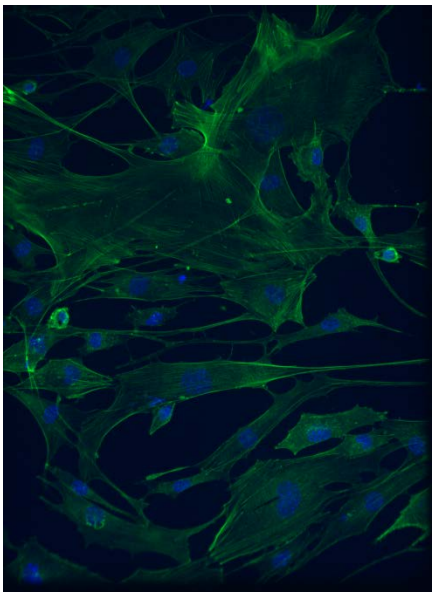	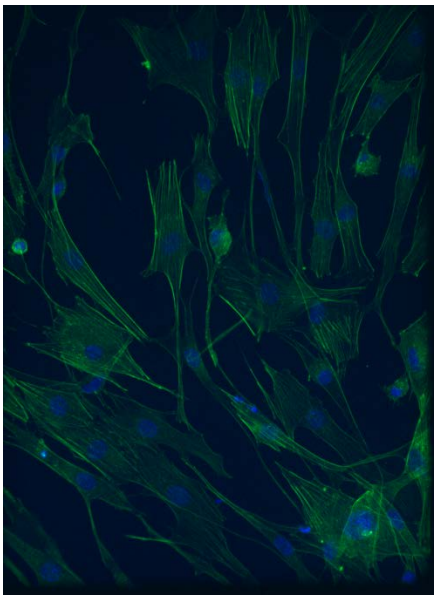

MMP-13

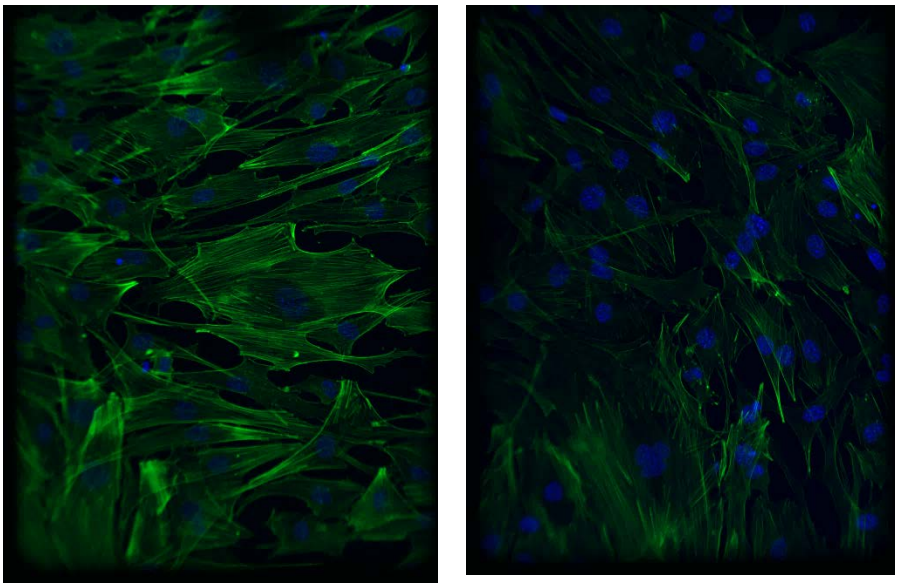

Figure A.3. Images (20x objective) of cover slips stained with DAPI and Phalloidin and treated with 10 nM of MMP-1, 2, 8, or 13 for 3 days.

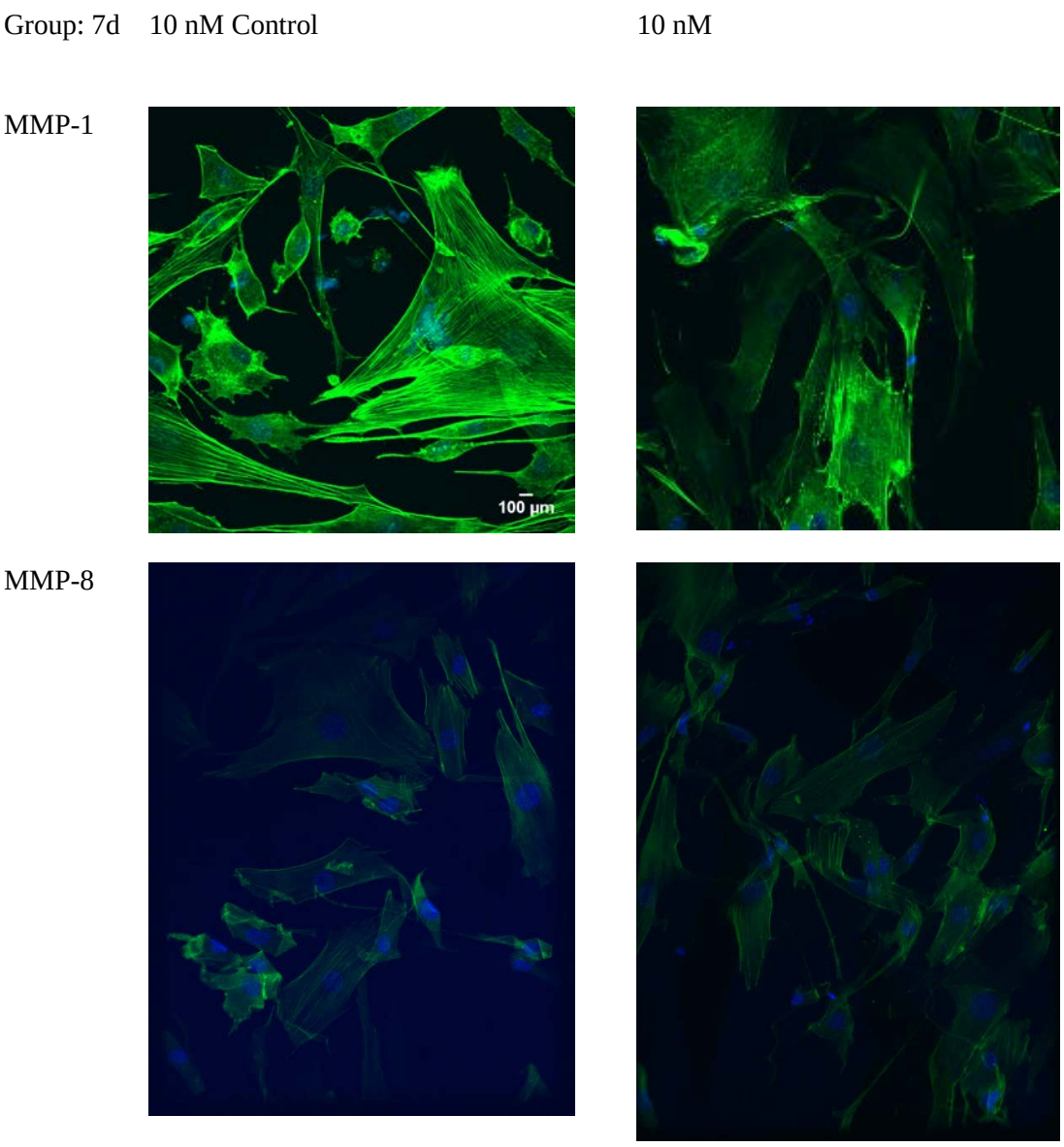

Figure A.4. Images (20x objective) of cover slips stained with DAPI and Phalloidin and treated with 10 nM of MMP-1 and MMP-8 for 7 days.

Appendix B. Supplemental Tables

Table B.1: P values from Figure 4.6. Statistical significance determined by $p < 0.05$.

Mechanical Property	TGFβ2 Only	MMP-2 with TGFβ2
Stiffness	0.744503945	0.788264615
Elastic Modulus	0.406750563	0.758677961
Stress	0.213514	0.8601517
Strain	0.4379985	0.4315197
Cross Sectional Area	0.497558	0.528672

Appendix C. Fiberfit and Image Post Processing

William Miller's Description of Post Processing Image Analysis

The extraction of modified k-values from the multimodal distributions in frequency versus angle space is performed by first using a Gaussian kernel density estimation to find a probability density function which fits the distribution using the stats module of the SciPy library. The peaks are then extracted from the PDF using the signal module of SciPy, with a minimum separation of 5 samples. The peaks are then threshold-filtered at 60% of the highest peak, and the highest 4 peaks are selected (to maintain consistent relative error across groups). A normal distribution is then fit under each peak that satisfies the threshold filter. Finally, by weighting the height of the fitted normal distribution by $1 - \frac{w}{180}$ where w is the width, in degrees, at 85% height, a modified k-value is determined. The modified k-values are then averaged across the group to generate a single modified k-value for the entire distribution.

Python Code

```
import matplotlib.pyplot as plt
from matplotlib.backends.backend_pdf import PdfPages
import ntpath
import pandas as pd
import numpy as np
from scipy import stats, signal
import os, sys, argparse

def modified_k(curve, x, idx):
        minima = signal.argrelmin(curve)[0]
        for ii, e in enumerate(minima):
                if e > idx:
                        l = minima[ii - 2]
                        h = minima[ii]
        slice = curve[l:h]
        for s in np.linspace(10, 1e-5, 25):
                p = stats.norm.pdf(x[l:h], x[idx], s)
                if (max(p) != 0.0) :
                        p *= curve[idx] / max(p)
                        if sum(p - slice) < 0:
                                break
        for i, e in enumerate(p):
                if e > 0.85 * max(p):
                        s = x[np.argmax(p)] - x[i]
                        break
        w = 1 - (2 * s) / (np.pi / 2.0) if 2 * s <= np.pi / 2 else 1
        return curve[idx] * w

parser = argparse.ArgumentParser()
parser.add_argument("--files", nargs="+", type=str)
```

```
vm = parser.parse_args()
pdf = PdfPages('plots.pdf')
columns = []
mdf = pd.DataFrame()

n = len(vm.files)
odf = pd.DataFrame(columns = ['Name', 'Modified k'])
sys.stdout.write("Progress: {:3d}%\r".format(int(0 / n) * 100))
for idx, file in enumerate(vm.files):
	sys.stdout.write("Progress: {:3d}%\r".format(int((idx + 1) / n * 100)))
	sys.stdout.flush()
	df = pd.read_csv(file)
	e = df['Angle'].values
	h = df['Normalized Power'].values
	l = len(e)
	e = np.hstack([e-np.pi, e, e+np.pi])
	h = np.hstack([h, h, h])
	columns.append((ntpath.basename(file), 'Angle'))
	columns.append((", "Normalized Power"))
	mdf = pd.concat([mdf, df], axis=1, sort=False)
	resample = np.random.choice(e, size = 400000, p = h / h.sum())
	rkde = stats.gaussian_kde(resample, 0.015)
	p = rkde.pdf(e)[:]
	kmod = 0.0
	nk = 0.0
	peaks = signal.find_peaks(p, distance = 5)[0]
	fpeaks = []
	for ii in peaks:
		if ii > l and ii < len(e) - l:
			fpeaks.append(ii)
	fpeaks = np.array(fpeaks)
	for peak in fpeaks[p[fpeaks].argsort()][-4:]:
		if (peak >= l and peak < len(e) - l) and p[peak] > 0.6*max(p):
			kmod += modified_k(p, e, peak)
			nk += 1.0
			plt.vlines(e[peak], 0, p[peak]*3.0, color = 'k')
	kmod = modified_k(p, e, np.argmax(p)) if nk == 0.0 else kmod / nk
	odf.loc[len(odf)] = [ntpath.basename(file), kmod]
	plt.bar(e, h, width = np.pi / (e.shape[0] / 3.0 - 1), fc = tab20[1])
	plt.plot(e, rkde.pdf(e)*3.0, dashes=[0.01, 2], lw=2, c='k')
	plt.xlim([0, np.pi])
	plt.xticks(np.linspace(0, np.pi, 19), np.linspace(0, 180, 19))
	plt.title(ntpath.basename(file))
	plt.figtext(0.9, 0.9, 'k = {:5.3f}'.format(kmod), ha='center', va='center')
	pdf.savefig(plt.gcf())
	plt.clf()

print()
odf.to_csv('kmod.csv', index=False)
```

```
mdf.columns = pd.MultiIndex.from_tuples(columns)
mdf.to_csv('output.csv', index=False)
pdf.close()
```